The Astronomical Journal, 131:2986–3007, 2006 June

CONTACT BINARIES WITH ADDITIONAL COMPONENTS. I. THE EXTANT DATA

Theodor Pribulla
Astronomical Institute, Slovak Academy of Sciences, 059 60 Tatranská Lomnica, Slovak Republic; pribulla@ta3.sk

and

Slavek M. Rucinski
David Dunlap Observatory, University of Toronto, P.O. Box 360, Richmond Hill, ON L4C 4Y6, Canada; rucinski@astro.utoronto.ca
Received 2005 September 1; accepted 2006 February 25

ABSTRACT

We have attempted to establish observational evidence for the presence of distant companions that may have acquired and/or absorbed angular momentum during the evolution of multiple systems, thus facilitating or enabling the formation of contact binaries. In this preliminary investigation we use several techniques (some of them distance-independent) and mostly disregard the detection biases of individual techniques in an attempt to establish a lower limit to the frequency of triple systems. While the whole sample of 151 contact binary stars brighter than $V_{\max} = 10$ mag gives a firm lower limit of 42% ± 5%, the corresponding number for the much better observed northern-sky subsample is 59% ± 8%. These estimates indicate that most contact binary stars exist in multiple systems.

Key words: binaries: close — binaries: eclipsing — stars: variables: other

Online material: machine-readable table

1. INTRODUCTION

The formation of binary stars is a fascinating subject generating a very active research effort. Separate conferences (Zinnecker & Mathieu 2001) are devoted to this subject, while specialized review papers (Tholine 2002; Zinnecker 2002; Bate 2004) describe difficulties in our understanding of this complex process. Binaries with orbital periods of the order of hundreds of days are usually considered as close in this context. We have no idea how short-period binaries with periods much shorter than 3–5 days form. In fact, such binaries, particularly those with periods shorter than 1 day, should not exist: indeed, even if some unknown process formed contact binaries at the T Tauri stage, the relatively large sizes of the component stars would imply that the resulting orbital periods be longer than about 3–5 days.

Formation in triple (or multiple) systems may alleviate the close-binary formation difficulty by allocating most of the angular momentum to the most distant component of a triple/multiple system, leaving a low angular momentum remnant. Such a scenario would have important observational consequences because, in observing close binaries, we would preferentially select stars with distant companions. One particular mechanism involving the Kozai cycles (Kozai 1962) may produce close binaries by invoking a very strong tidal interaction during periastron passages when the inner, close (low angular momentum) orbit is perturbed by the third body into a very eccentric one. The close periastron interactions may then lead to a rapid angular momentum loss (Kiseleva et al. 1998; Eggleton & Kiseleva-Eggleton 2001).

A confirmation of the triple-body formation of very close binaries can only come through observations and careful statistical investigations. Unfortunately, proving or disapproving this hypothesis is difficult and, as for all statistical studies, is hindered by observational bias and selection effects. In this paper we limit our scope to contact binaries, the most extreme objects with the lowest angular momentum content among all main-sequence (MS) binary stars. Contact binaries (Rucinski 1993) are made of solar-type stars with spectral types ranging from early K through G and F to middle A; they have short orbital periods ranging from 0.22 to about 0.7 days, at which point the statistics become unreliable and the properties of massive contact binaries become less well defined. Thus, in spite of the unquestioned existence of very massive contact binaries, it is not clear whether a continuous sequence joins the solar-type contact binaries (stars also known as W UMa–type variables) with the early-type B and O-type binaries. In this paper we limit ourselves to binaries with periods shorter than 1 day, which is the traditional period limit for the solar-type (W UMa–type) contact binaries.

Rucinski & Kaluzny (1982) commented on a high incidence of visual binaries among contact binaries while discussing a visual binary consisting of two W UMa–type systems, BV Dra and BW Dra. Later on, Chambliss (1992) listed several cases of triple systems with contact binaries in his compilation, and Hendry & Mochnacki (1998) detected a few cases of triple systems. However, these were fragmentary, almost anecdotal observations, and there clearly exists a need to quantify the matter of the multiplicity of very close binaries.

This paper attempts to characterize all indications of triplicity and/or multiplicity by categorizing contact systems into those with "detected," "suspected," and "nondetected" companions, with an additional obvious category of "not observed." The techniques actually used are described in §§ 3–5. Not all techniques discussed by us are equally useful, and not all imaginable techniques have been considered; there is still a lot of room for expansion. Also, types of companion are not explicitly discussed in the paper, as our goal was simply to summarize the extant information irrespective of what accompanies a given contact binary. Thus, a huge subject of selection effects and biases is only glanced over in this paper. Future studies, such as Paper II of this series, on spectroscopic detection in spectra used for the David Dunlap Observatory (DDO) radial velocity program (D'Angelo et al. 2006, hereafter Paper II), will more fully address specific limitations of various detection techniques.

We describe our sample in § 2. The main results of this paper are described in §§ 3–5 and summarized in Table 1, where we collect all partial results and attempt to combine "suspected" cases into detections. Results for individual cases are summarized

TABLE 1

MULTIPLICITY OF CONTACT BINARY STARS: SUMMARY DATA

NAME	NOTE	V_{max}	WDS	θ (deg)	ρ (arcsec)	d (AU)	ΔV	HIP	σ_π	σ_μ	β	ΔRV	P_3 (yr)	$a \sin i$ (AU)	ϵ_{BV}	$\log X$	MOON	FLAGS 1234 5678	WEIGHT	TRIPLE
Binaries Brighter than $V = 10$																				
AB And	*	9.50	CFHT98	306	18.90	2266	7.3	−S	1.48	2.69			59	3.8	0.45	−3.58	...	NPSN NDNN	2	Y
BX And		8.90	02091+4048	60	19.70	4195[a]	1.37	CC	2.93	1.41			62	2.2	0.27	−4.24	...	P−SN −SNN	1.5	Y
CN And		9.70						−−		1.56					0.27	−3.52	...	N−−N NNNN	0	
GZ And	*	9.92	02122+4440	33	2.13	353[a]	2.4	−S		2.76	0.02				0.19		...	DDSN D−NN	3.5	Y
V376 And		7.63						−−	0.89	2.76					0.17		...	N−NS N−NN	0.5	
V395 And		7.55	23445+4623	103	5.64	2541[a]	2.50	CA	1.12	1.77					−0.12		...	P−NN −−SN	1	Y
S Ant		6.40						−−	0.71	2.06					0.19		...	N−NN −−NN	0	
HV Aqr		9.71						−−		2.05	0.02				0.11	−3.63	...	N−−N DNNN	1	Y
OO Aql		9.20						−−		2.19					0.56	−3.49	...	N−−N −NNL	0.5	
V1464 Aql		8.60						−−	1.26	1.84					0.15		...	N−NN −−NN	0	
V535 Ara		7.17						−−	0.90	2.05					0.19		...	N−NN −−NN	0	
V851 Ara		6.86						−−	0.82	1.41					0.12	−4.93	...	N−NN −−NN	0	
V867 Ara		7.39	17424−4618	316	0.36	55[a]	1.14	CA	2.62	1.84					−0.10		...	D−NN −−SN	1.5	Y
V870 Ara		8.80						−−	1.34	2.05					0.34		...	N−NN −−NN	0	
V402 Aur		8.84						−−	1.31	1.35					0.27		...	N−NN N−NN	0	
V410 Aur	*	9.94	05012+3430	229	1.70	345[a]	1.04	CA	5.39	8.41	0.26	9			0.18	−3.79	...	D−NS D−NN	2.5	Y
44 Boo	*	4.71	15038+4739	49	1.70	22	0.78	CB	1.03	1.70	1.74	−17			−0.23	−4.25	...	D−NN DNSN	2.5	Y
CK Boo	*	8.99	CFHT98	196	0.12	15[a]	2.8	−−	1.34	2.12	0.01		21	5.0	0.08	−3.94	...	NDNN DSNN	2.5	Y
DW Boo		7.38						−−	1.11	2.26					−0.04		...	N−NN −−SN	0.5	
EF Boo		9.27						−−	1.06	1.63					0.20	−3.90	...	N−NN N−NN	0	
FI Boo		9.43						X−	2.10	1.77	0.01				0.30	−3.76	...	N−DN D−NN	2	Y
AO Cam	*	9.50						−−		3.18	0.01				0.19	−3.98	...	N−−N DNNN	1	Y
DN Cam		8.15						−S	0.89	1.98					0.11	−4.58	...	N−SN N−NL	1	Y
FN Cam		8.50						−−	0.95	1.70					0.25		...	N−NN N−NN	0	
BO CVn		9.48						−−		1.56					0.12		...	N−−N −NNN	0	
IS CMa		6.84						−−	0.71	1.27					0.19		...	N−NN −−NN	0	
BH CMi		9.30						−−		1.70					0.07		...	N−−N −NNN	0	
V776 Cas		8.82	01534+7003	137	5.38	885[a]	2.00	CA	1.56	2.12		−2			0.14		...	D−NN N−NN	1	Y
RR Cen		7.27						−−	0.85	1.91					0.21		...	N−NN −−NN	0	
V752 Cen		9.10						−S	1.47	1.98					0.17	−3.79	...	N−SN −−NN	0.5	
V757 Cen		8.30						−−	1.10	1.98					0.15	−3.83	...	N−NN −−NN	0	
V758 Cen		9.48						−−	1.55	2.12					−0.10		...	N−NN −−SN	0.5	
V759 Cen		7.40						−−	0.93	1.35					0.21	−3.74	...	N−NN −NNN	0	
V839 Cen		9.51						−−	1.66	1.84					0.16	−3.47	...	N−NN −−NN	0	
VW Cep	*	7.23	20374+7536	291	0.50	14	2.80	CC	0.97	1.84	0.06		28	2.3	0.11	−3.56	...	D−SN −DNN	2.5	Y
EM Cep	*	7.02	21538+6237	145	62.60	49722[a]	0.84	−S	0.55	2.05					0.10		...	N−SN −NNN	0.5	
V445 Cep		6.81						−−	0.50	1.98	0.06				−0.12		...	N−NN D−SE	2	Y
AA Cet		6.56	01590−2255	303	8.56	740[a]	0.36	CB	2.36	2.62	0.59				0.22		...	D−NS −−NN	1.5	Y
CL Cet		9.77						X−	3.63	2.05					0.20		...	N−DN −−NN	1	Y
CT Cet		9.41	01098−2013	30	3.58	308[a]	0.79	CA	4.01	3.70					−0.05	−4.24	...	D−NS −−NN	1.5	Y
DY Cet		9.42						−S	2.17	1.84					0.14	−3.94	...	N−SN −−NN	0.5	
EE Cet	*	8.64	02499+0856	194	5.66	902[a]	0.07	CA	4.89	4.74					0.12	−3.90	...	D−NS N−NN	1.5	Y
DO Cha		7.61						−−	0.57	1.63					0.36	−3.38	...	N−NN −−NL	0.5	
RS Col		9.54						−−	1.28	2.48					0.46	−4.01	...	N−NN −−NL	0.5	

TABLE 1—*Continued*

Name	Note	V_{max}	WDS	θ (deg)	ρ (arcsec)	d (AU)	ΔV	HIP	σ_π	σ_μ	β	ΔRV	P_3 (yr)	$a \sin i$ (AU)	ϵ_{BV}	$\log X$	Moon	Flags 1234 5678	Weight	Triple
Binaries Brighter than $V = 10$																				
KR Com		7.13	13203+1746	8	0.10	8	0.6	−−	0.87	1.56	0.56	4			0.22	−3.98	...	D−NN D−NN	2	Y
eps CrA		4.74						−−	0.92	1.06					0.21	−5.68	...	N−NN −−NN	0	
YY CrB		8.48						−−	0.85	2.26					0.20	−3.64	...	N−NN NNNN	0	
SX Crv		8.99						−−	1.21	1.98					−0.09	−3.57	...	NNNN NNSN	0.5	
DT Cru		9.91						−S	1.70	4.17					0.27		...	N−SS −−NN	1	Y
V1073 Cyg		8.23						−−	0.95	2.05					0.31		...	NNNN NNNN	0	
V2082 Cyg		6.63						−−	0.56	1.84	0.03				0.23	−4.74	...	N−NN D−NL	1.5	Y
V2150 Cyg		8.00	21182+3035	210	3.68	667[a]	3.35	CA	1.59	1.77					0.08		...	D−NN N−NN	1	Y
LS Del		8.61						−−		1.27					0.10	−4.09	...	N−−N NNNN	0	
AP Dor		9.27						−−	0.92	2.12					0.14	−4.11	...	N−NN −−NN	0	
BV Dra	*	7.88	15118+6151	353	16.10	1083	0.69	CA	2.56	1.70					0.07	−3.53	...	D−NN −NNN	1	Y
BW Dra	*	8.61	15118+6151	353	16.10	1089[a]	0.69	CA	5.18	4.46					0.01	−3.29	...	D−NS −NNN	1.5	Y
GM Dra		8.66						−−	0.88	1.98					0.03	−3.95	...	N−NN N−NN	0	
YY Eri		8.10						−−	1.20	1.91					0.13	−3.79	...	NNNN −NNN	0	
BV Eri		8.12						−−	1.11	1.77					0.21		...	NNNN −−NN	0	
FP Eri		9.59						−−	1.28	1.70					0.01		...	N−NN −−NE	0.5	
FX Eri		9.56						CA	1.06	1.56					0.10	−3.60	...	N−NN −−NN	0	
V345 Gem	*	7.70	07385+3343	352	3.19	233[a]	1.40	CA	1.77	2.62					−0.39	−4.42	...	D−NN −−SN	1.5	Y
AK Her	*	8.29	17140+1621	323	4.20	425[a]	4	XS	2.77	1.77			58	1.7	0.21	−4.21	...	DDDN NDNN	4	Y
V842 Her		9.85						−−		2.83					0.21		...	N−−N N−NN	0	
V899 Her		7.82						−−	0.77	1.49	1.50	var			0.13	−4.41	...	N−NN D−NN	1	Y
V918 Her		7.31						−−	0.93	1.41					0.11		...	N−NN N−NN	0	
V921 Her		9.33						−−	0.97	1.84					0.22		...	N−NN N−NN	0	
V972 Her		6.62						−−	0.61	1.70					0.14	−5.14	...	N−NN N−NN	0	
V1003 Her		9.69						−−	1.57	1.49					0.18		...	N−NN −−NN	0	
TU Hor		5.90						−−	0.56	0.99					0.06		...	N−NN −−NN	0	
WY Hor		9.39						−−	1.00	1.56					0.36	−3.75	...	N−NN −−NN	0	
FG Hya		9.90	CFHT98	145	16.50	2602[a]	4	−−	1.90	1.84					0.05	−3.82	...	NPNN NNNN	0.5	
PP Hya		6.78						−−	0.93	1.84					0.08		...	N−NN −−NN	0	
CE Hyi		8.36	01389−5835	9	2.00	420[a]	0.37	CA	2.01	5.10					0.08		...	D−NS −−NN	1.5	Y
CN Hyi		6.56	02456−7114	132	0.51	30	3.76	CA	0.65	1.70					0.18	−4.88	...	D−NN −−NN	1	Y
CP Hyi		7.80						−−	0.60	1.49					0.12		...	N−NN −−NN	0	
SW Lac	*	8.51	CFHT98	85	1.70	138	2.54	−S	1.26	1.84	0.01	sim	28	2.6	0.20	−3.40	...	NDSN DDNN	3.5	Y
V407 Lac		8.29						−−	0.93	1.49					−0.05		...	N−NN −−SN	0.5	
UZ Leo		9.58						−S	1.59	1.56					0.23		M	NNSN NNNN	0.5	
XY Leo	*	9.45						−S	1.80	1.56	0.10	var	20	4.1	0.29	−3.23	M	NNSN DDNN	2.5	Y
AM Leo	*	9.25	11022+0954	270	11.50	883	1.68	CA	3.64	1.91					0.10	−4.00	M	D−NN −NNN	1	Y
AP Leo		9.32						−S	1.70	2.40					0.20	−3.89	M	NNSN NNNN	0.5	
ET Leo		9.44						−S	1.44	1.41	0.02				0.18	−3.72	...	N−SN D−NN	1.5	Y
EX Leo		8.13						−−	1.11	1.27					0.15	−3.89	...	N−NN N−NN	0	
VW LMi	*	7.93						−−	0.90	1.63	0.42	var			0.13		...	N−NN D−NN	1	Y
ES Lib		7.11	15168−1302	174	0.20	25	?	−S	0.91	1.13					0.15	−4.64	M	D−SN −−NN	1.5	Y
FT Lup		9.70						−−		2.69					0.19		...	N−−N −NNN	0	
UV Lyn		9.41						−−	1.62	2.55					0.34	−3.99	...	NNNN NNNN	0	
TY Men		8.08						−−	0.63	1.63					0.01		...	N−NN −NNN	0	

TABLE 1—*Continued*

Name	Note	V_{max}	WDS	θ (deg)	ρ (arcsec)	d (AU)	ΔV	HIP	σ_π	σ_μ	β	ΔRV	P_3 (yr)	$a \sin i$ (AU)	ϵ_{BV}	$\log X$	Moon	Flags 1234 5678	Weight	Triple
Binaries Brighter than $V = 10$																				
AN Men		9.24						––	0.86	1.98					0.21		...	N–NN ––NN	0	
V752 Mon	*	6.90	07079−0441	26	1.71	213[a]	0.51	CA	1.40	4.17					0.06		...	D–NS ––NN	1.5	Y
V753 Mon		8.21						––	1.04	1.35					0.24		...	N–NN N–NN	0	
V2 Mon		9.90						––		2.48					0.21	−3.98	...	N––N ––NN	0	
V3 Mon		8.90						––		1.63					0.09		...	N––N ––NN	0	
DE Oct		9.09	20194−7608	128	22.90	5423[a]	2.85	––	1.03	1.98					0.17		...	P–NN ––NN	0.5	
V502 Oph	*	8.34						––	1.17	1.56	0.01	sim			0.38	−3.86	...	NNNN DNNN	1	Y
V566 Oph		7.46						––	1.11	1.70			23	1.2	0.11	−4.40	...	NNNN NDNN	1	Y
V839 Oph		8.80	CFHT98	8	8.20	1014	6.1	––	1.44	2.62					0.26	−3.70	...	NDNS NNNN	1.5	Y
V1010 Oph		6.04						––	0.83	1.13					0.10	4.66	...	N–NN N–NN	0	
V2377 Oph		8.45						––	1.22	2.62					0.29	−3.74	...	N–NS N–NN	0.5	
V2388 Oph	*	6.14	17542+1108		0.09	6	0.2	G–	0.81	1.63	0.20	−5			0.34		...	D–DN D–NN	3	Y
ER Ori		9.28	05112−0833	354	0.19	31[a]	1.99	G–	2.16	1.84			52	5.7	0.24	−4.27	...	DDDN –SNN	3.5	Y
V1387 Ori		8.71	06094+1711	12	3.19	1003[a]	3.48	CC	2.23	1.41					0.10		...	D–SN ––NN	1.5	Y
MW Pav		8.63						––	1.08	1.56					0.26		...	N–NN ––NN	0	
V386 Pav		8.28						––	1.01	1.98					0.12		...	N–NN ––NN	0	
U Peg		9.23	CFHT98	275	4.05	564	5.2	––	1.43	1.56					0.23	−3.94	...	NDNN –NNN	1	Y
KP Peg		7.05	21267+1341	217	3.46	637[a]	1.77	CA	1.67	2.55	0.22				−0.02	−4.76	...	D–NS D–SN	3	Y
KS Peg		5.45	23379+1824	246	27.70	2029	5.20	––	0.75	1.27					−0.19		...	P–NN N–SN	1	Y
V335 Peg		7.23						––	0.86	1.91					0.38	−4.16	...	N–NN N–NL	0.5	
V351 Peg		7.92						––	0.92	1.35					0.14	−4.60	...	N–NN N–NN	0	
V353 Peg		7.41						G–	0.89	1.77					0.08		...	N–DN ––NN	1	Y
V357 Peg		8.91						––	1.21	1.27					0.19		...	N–NN ––NN	0	
V2 Peg		9.50						––		1.41					0.20		...	N––N ––NN	0	
IW Per		5.76						––	0.81	1.70					0.08		...	N–NN N–NN	0	
V579 Per		7.78						––	0.89	1.77					0.01		...	N–NN ––NN	0	
V592 Per		8.19	04445+3953	194	0.21	39[a]	0.85	CA	1.55	1.49	0.60	1			0.39		...	D–NN D–NN	2	Y
AE Phe		7.56						––	0.81	1.35					0.21	−3.80	...	N–NN –NNN	0	
BM Phe		9.16						––	1.17	1.78					0.09		...	N–NN ––NN	0	
TV Pic		7.37						––	0.63	1.49					0.08		...	N–NN ––NN	0	
AQ Psc		8.60	01211+0736	64	26.20	3263	2.8	–S	1.29	2.12					0.26	−3.85	M	PPSN N–NN	1.5	Y
TY Pup		8.40	CFHT98	2	8.40	4264		––	1.01	1.98					0.30		...	NPNN ––NN	0.5	
RZ Pyx		8.94						––	1.06	2.05					−0.17		...	N–NN ––SN	0.5	
V701 Sco		8.63						––	1.31	1.84					−0.02		...	N–NN ––NN	0	
V1084 Sco		8.92						––	1.32	2.13					0.14	−4.34	...	N–NN ––NN	0	
OU Ser		8.10						––	0.95	1.56					−0.04	−3.69	...	N–NN N–SN	0.5	
Y Sex		9.83	10028+0106	154	0.49	121[a]	2.62	CB	3.38	1.98					0.10		...	D–NN –NNN	1	Y
VY Sex		9.01						––		1.49					0.31	−3.92	...	N––N N–NN	0	
V781 Tau		8.56	CFHT98	163	8.00	650	8	––	1.35	1.49					0.13	−3.47	M	NDNN –NNN	1	Y
V1123 Tau		9.70	03350+1743	135	4.27	571[a]	1.73	CA	5.37	4.53					0.47	−3.55	M	D–NS ––NN	1.5	Y
V1128 Tau		9.46	03495+1255	196	12.10	1310[a]	1.08	CA	4.77	1.77					0.05	−3.95	...	D–NN ––NN	1	Y
AQ Tuc		9.91						––	1.24	2.27					0.21		...	N–NN ––NN	0	
DX Tuc		9.47						––	1.12	2.26					0.13		...	N–NN ––NN	0	
W UMa		7.75	09438+5557	43	6.40	317	4.45	–S	1.05	1.70					0.10	−3.79	...	D–SN SNNN	1.5	Y

TABLE 1—*Continued*

Name	Note	V_{max}	WDS	θ (deg)	ρ (arcsec)	d (AU)	ΔV	HIP	σ_π	σ_μ	β	ΔRV	P_3 (yr)	$a \sin i$ (AU)	ϵ_{BV}	log X	Moon	Flags 1234 5678	Weight	Triple
Binaries Brighter than $V = 10$																				
AW UMa	*	6.83	11301+2958	33	67.20	4442	2.5	––	0.90	1.27			17	0.4	0.08		...	P–NN SDNN	1.5	Y
HN UMa		9.75						––	1.39	2.62					0.11	−3.80	...	N–NN N–NN	0	
HV UMa		8.52						––	1.23	1.84					0.17		...	N–NN ––NN	0	
HX UMa		8.75	12021+4304	86	0.63	78[a]	3.31	CB	3.01	1.56	0.05	−4			0.09	−4.45	...	D–NN D–NN	2	Y
II UMa		8.04	12329+5448	9	0.87	178[a]	1.64	CA	1.81	1.98	0.17	−8			0.34		...	D–NN D–NN	2	Y
TU UMi		8.73	14557+7618	141	0.22	46[a]	0.47	CA	0.97	1.70	1.25				0.02		...	D–NN D–NN	2	Y
TV UMi	*	8.62						––	0.78	1.70	0.90	var			0.27	−4.31	...	N–NN D–NN	1	Y
OQ Vel		7.67	08464−5251	334	0.10		0.50	––	0.62	2.13					0.18	−4.57	...	N–NN ––NN	0	
LL Vel		6.72			<0.03	19		–S	0.60	1.41					0.04	−5.40	...	D–SN ––NN	1.5	Y
V353 Vel		6.79						––	0.83	1.63					−0.01		...	N–NN ––NN	0	
AG Vir		8.35						––	1.18	1.49	0.05	sim			0.15		...	NNNN DNNN	1	Y
AH Vir	*	8.89	12143+1149	16	1.73	174[a]	3.00	CC	3.11	1.84	0.11		41	4.2	0.39	−3.59	...	DDSN DDNN	4.5	Y
CX Vir		9.80						––		2.12					0.40		M	N––N ––NN	0	
FO Vir		6.50	13298+0106	336	22.80	1926	6.4	–S	0.85	1.49					0.19	−5.08	...	D–SN N–NN	1.5	Y
GR Vir		7.80						––	1.18	1.63					0.07	−3.93	...	NNNN NNNN	0	
HT Vir	*	7.06	13461+0507	163	0.56	36	0.63	CB	2.72	2.26	1.06	var			0.21	−4.03	...	D–NN D–NN	2	Y
MW Vir		6.93						––	0.91	1.27					0.03	−4.33	...	N–NN ––NN	0	
NN Vir		7.60						––	1.14	2.05					0.14		...	N–NN N–NN	0	
Binaries Fainter than $V = 10$																				
AH Aur		10.20	CFHT98	63	3.20	518	4.20	–S	2.05	2.40					0.37	−3.71	M	NDSN NNNN	1.5	Y
TY Boo		10.81						––		6.15			56	4.1	0.07		...	N––S –SNN	1	Y
TZ Boo		10.41	CFHT98	120	10.60	1885[a]	6.90	––	1.49	1.84			34	6.3	−0.05		...	NDNN –DSE	3	Y
TX Cnc		10.00	08400+1900	25	25.10	3765[a]	2.4	––		1.77					0.36	−3.89	M	P––N NNNN	0.5	
AH Cnc	*	13.31	08517+1151	273	26.80	23970[a]	0.24	––								−3.63	...	N––– ––NN	0	
V523 Cas		10.62						––		3.61			86	4.8	−0.28	−3.51	...	N––N NSSN	1	Y
GW Cep		11.40						––		2.90			14	0.7	−0.05		...	N––N –DSN	1.5	Y
TW Cet		10.43	01489−2053	296	8.79	1588[a]	1.99	CB	3.50	3.47					0.07	−3.52	...	D–NN ––NN	1	Y
RW Com		11.00						–S	2.45	3.54					0.06	−3.82	...	NNSN –NNN	0.5	
CV Cyg		10.80	19543+3803	140	0.70	787[a]	0.02	––		2.40					0.34		...	D––N ––NN	1	Y
DK Cyg		10.37						–S	1.78	2.19					0.17		...	NNSN NNNN	0.5	

TABLE 1—*Continued*

Name	Note	V_{max}	WDS	θ (deg)	ρ (arcsec)	d (AU)	ΔV	HIP	σ_π	σ_μ	β	ΔRV	P_3 (yr)	$a \sin i$ (AU)	ϵ_{BV}	$\log X$	Moon	Flags 1234 5678	Weight	Triple
Binaries Fainter than $V = 10$																				
V401 Cyg		10.64	CFHT98	359	18.00	9262[a]	1.2	X–	8.04	2.62	0.03	sim			0.17		...	NPDN D–NN	2.5	Y
V700 Cyg		11.90	20311+3847	74	21.60	6317[a]	1.5	––									M	P––– ––NN	0.5	
EF Dra		10.48	18055+6945	240	2.40	807[a]	1.19	––		3.68	0.20	4			0.18	−3.82	...	D––N DNNN	2	Y
UX Eri		10.50						–S	2.84	3.18			43	3.9	0.36	−3.30	...	NNSN NSNN	1	Y
QW Gem		10.18	06508+2927	26	6.38	1567[a]	1.16	CA	5.42	2.69					0.07	−4.04	...	D–NN N–NN	1	Y
V829 Her		10.10						––		4.03			11	0.9	0.11	−3.76	...	N––S NSNN	1	Y
XZ Leo		10.18	CFHT98	112	18.30	5801[a]	7	–S	1.71	1.70					0.19		M	NPSN NNNN	1	Y
VZ Lib		10.13						––	1.96	2.55	0.20	var			0.33		M	NNNN D–NN	1	Y
V532 Mon		12.20	07020−0018	179	10.90	10035[a]	0.1	––		2.48							...	P––N ––NN	0.5	
V508 Oph		10.06	CFHT98	19	2.40	419[a]	3.9	–S	2.14	2.19					0.13	−3.92	...	NDSN –NNN	1.5	Y
V1363 Ori		10.22						–S	2.36	1.41					0.30		...	N–SN N–NN	0.5	
BB Peg	*	10.80						––	2.26	2.69	0.01		21	0.8	0.09			NNNN DSNN	1.5	Y
KN Per		11.52						––	3.49	2.48					0.29		...	N–NN ––NN	0	
BQ Phe		10.32						–S	2.08	2.33					0.27		...	N–SN ––NN	0.5	
CW Sge		11.13						XS	4.14	2.26					0.28		...	N–DN ––NN	1	Y
BE Scl		10.24						X–	5.11	2.48					0.29		...	N–DN ––NN	1	Y
RS Ser		10.80						––		2.33					0.39	−3.52	...	N––N ––NL	0.5	
RZ Tau		10.08	CFHT98	43	0.80	139[a]	3.7	–S	1.85	1.84					0.11		...	NDSN –NNN	1.5	Y
EQ Tau		10.50						––		2.05			50	3.9	0.38		M	N––N NSNN	0.5	

Notes.—Name: The GCVS designation. Note: An asterisk indicates a comment in Table 3. V_{max}: Johnson or transformed *Hipparcos* H_p maximum magnitude. WDS: Designation of the system (if it is a visual binary or common-proper-motion pair) in the most recent online version of the WDS (http://ad.usno.navy.mil/wds/wds.html) or CFHT indicating a new detection, as given in Table 4. θ: Position angle of the secondary (=fainter) component in degrees. ρ: Angular separation of the components in arcseconds. d: Projected separation in astronomical units computed from angular separation and the *Hipparcos* parallax. ΔV: Visual brightness difference of the components. HIP: *Hipparcos* flags H59 and H61 (H59 shows the type of astrometric solution: C, linear motion; G, acceleration term necessary, i.e., very probably an astrometric binary; X, stochastic solution, i.e., very probably an astrometric binary with $P < 3$ yr; H61 shows the quality of the orbital solution: grades ABCD [A = best] or suspected nonsingle, S. σ_π: *Hipparcos* parallax error in milliarcseconds. $\sigma_\mu = \{[\sigma(\mu_\alpha)\cos\delta]^2 + \sigma^2(\mu_\delta)\}^{1/2}$: Proper-motion error in the Tycho-2 catalog. β: Ratio of apparent luminosities $l_3/(l_1 + l_2)$ determined from broadening functions (see the text). ΔRV: Difference between the third component velocity and the systemic velocity of the underlying binary in kilometers per second; "sim" signifies similar velocities, and "var" signifies that the third component has a variable velocity. P_3: Orbital period of the third component as determined from LITE. $a \sin i$: Semimajor axis of the eclipsing pair around the common center of gravity in astronomical units determined using the LITE. ϵ_{BV}: Difference between observed Tycho-2 $B - V$ color index and the SPBE (see the text). $\log X = \log f_X/f_{bol}$: Flux ratio of the X-ray flux from the RASS to the bolometric flux (see § 4.3). Moon: "M" signifies that the system can be occulted by the Moon (within 5°9′ from the ecliptic). Flags: Explained in Table 2. Weight: Sum of weights of individual detection techniques (any detection counts with weight 1.0 and any possibility or suspicion with 0.5). Triple: Our final evaluation of triplicity; "Y" = yes if the sum of weights is equal to or larger than 1.0. Systems without GCVS designations are V2 Mon = TYC 4824−00153-1, V3 Mon = TYC 4835−01947-1, and V2 Peg = TYC 1720−00658-1.Table 1 is also available in machine-readable form in the electronic edition of the *Astronomical Journal*.

[a] Distance estimated using the absolute magnitude calibration of Rucinski & Duerbeck (1997) or using other methods (see text). This is done if the relative error of the parallax is larger than 0.2 or if the parallax is negative.

TABLE 2

EXPLANATION OF FLAGS FOR DIFFERENT TYPES OF OBSERVATIONS

Flag	Definition
1	Visual binary present in the WDS (DPN). "D" for systems with a projected separation less than 2000 AU, "P" for systems with a separation between 2000 and 20,000 AU, and "N" for systems not present in the WDS Catalog or with a separation larger than 20,000 AU.
2	CFHT AO observations (DPN–. The flags are the same as for the WDS. "–" here means that the system was not observed.
3	H59 (CGX– and H61 (ABCS–) *Hipparcos* catalog flags. "D" if X or G in H59, "S" if S or C in H61.
4	σ_μ (SN–. "S" if proper-motion error higher than 3 σ from the median.
5	Spectroscopic detection (DSN–) Detection in broadening functions or through spectral features (DN–). Large changes of systemic velocity were coded by "S."
6	LITE indication (DSN–. D: a stable orbit with more than 1.5 cycles covered; "S": a somewhat unstable solution or less than 1.5 cycles covered; "–": less than 25 *pe* or CCD minima or the interval of observations <10 yr.
7	SPBE indication (SN–. "S" if the system is bluer than the corresponding blue envelope color.
8	RASS X-ray to visual flux ratio (LEN). "L" when a late-type companion is indicated by a large f_X/f_{bol} ratio in early-type contact binary, "E" when the ratio is below the lower envelope of detection limit, indicating an early-type third component, otherwise "N."

NOTES.—Flags applicable to a particular type of technique are given in parentheses. Generic names: D, detection; S, strong suspicion of detection; P, possibility of a companion; N, no detection; –, not observed or insufficient data.

TABLE 3

NOTES ON SELECTED CONTACT BINARIES

Name	Comments
AB And	The third component is clearly seen in the LITE but has not been detected during the CFHT AO observations.
GZ And	A multiple (trapezoidal) system, with colors and magnitudes indicating that all visual components may be physically associated. It does not have a *Hipparcos* parallax.
V410 Aur	The visual component, identical to that of the spectroscopic detection, shows RV variability, indicating that it is possibly SB1.
44 Boo	The closest contact binary. The 206 yr period of the visual orbit is reflected in the LITE but cannot be determined solely from this effect, so it is considered as *not detected* by the LITE.
CK Boo	The third component, detected independently by the LITE and CFHT AO observations, is very probably the same body. Krzesinski et al. (1991) detected a small but definite ultraviolet excess, so it is possible that the third component is a white dwarf.
AO Cam	A very preliminary LITE solution has been given by Qian et al. (2005). Spectral signatures of a companion detected by D'Angelo et al. (2006).
AH Cnc	A member of M67. A physical link within WDS 08517+1151 is uncertain.
VW Cep	The third component has been detected by several techniques. The visual and LITE orbits still show an additional wobble.
EM Cep	A member of the open cluster NGC 7160. The projected separation of the components (ρ/π) is almost 50,000 AU, which is much larger than for all remaining wide systems of this sample. Hence, it is not considered as a genuine triple system.
EE Cet	While the southern component of WDS 02499+0856 is a contact binary, unpublished DDO spectroscopic observations show that the northern component is a double-lined (SB2) binary and hence that it is a quadruple system.
BV Dra and BW Dra	A well-known quadruple system composed of two contact binaries. BW Dra shows additional astrometric complications.
V345 Gem	The contact binary is the fainter component of a visual double.
AK Her	The fainter visual component cannot be identified with the component indicated by the LITE, so the system is possibly a quadruple one.
SW Lac	Lines of the third component were detected spectrally by Hendry & Mochnacki (1998); this is probably the same component as seen in the CFHT AO data. The LITE indicates two companions, but the visual companion does not seem to correspond to any of the possible bodies suggested by the LITE solution.
XY Leo	A member of a quadruple system detected by Barden (1987). The companion binary is a BY Dra−type binary system. The LITE orbit is exceptionally well defined.
AM Leo	A member of a relatively wide visual binary. A marginally acceptable LITE solution for the contact binary was given by Qian et al. (2005).
VW LMi	A quadruple system according to DDO spectral observations (to be published). The companion binary has an orbital period of 7.93 days, while both binaries appear to revolve about the common center of gravity in 355 days.
V752 Mon	The contact binary is the fainter component of the visual double. The brighter primary is a rapidly rotating A-type star obliterating signatures of the contact pair in the spectra.
V502 Oph	Lines of a third component were detected by Hendry & Mochnacki (1998).
V2388 Oph	A visual binary with an orbital period of only 8.9 yr.
BB Peg	D'Angelo et al. (2006) detected M dwarf signatures in the spectrum. A LITE analysis indicates a compatible body with a minimum mass of 0.18 $M_\odot$.
AW UMa	A proper-motion pair with BD +30 2164. The projected separation of the components is $d = \rho/\pi = 4400$ AU. The magnitudes and colors indicate a physical link. The LITE and systemic velocities show additional perturbations that may be related to another, closer companion.
TV UMi	A quadruple system according to the DDO spectral observations (to be published). The second binary is a detached system with a highly eccentric orbit and a period of a few weeks.
AG Vir	The faint companion has been detected in the DDO spectra (to be published).
AH Vir	The visual companion cannot be identified with the component indicated by the LITE.
HT Vir	The components of WDS 13461+0507 revolving in 274 yr orbit are both binaries. While component B is a contact binary, component A is a single-lined binary (SB1) with $P = 32.45$ days (Lu et al. 2001).

in a condensed form in the column headed "Flags" by codes specific for each technique. The codes are explained in Table 2, while individual binaries requiring comments are listed in Table 3. Section 6 summarizes the main results of this study, while § 7 gives a discussion of possible directions for future work.

2. THE SAMPLE

Meaningful statistical results on stellar properties, including the matter of multiplicity, can only be properly studied utilizing volume-limited samples. Unfortunately, a proper volume-limited sample of contact binaries does not exist. In fact, as we describe below, we are very far from having even a good magnitude-limited sample.

As usual for stellar statistics based on diversified data, strengths and biases of various techniques tend to depend on brightness. We decided to set a limit for our sample at the magnitude $V_{\max} = 10$. This magnitude limit is a compromise between a sufficient size of the sample and a reasonable completeness. At this point we feel confident that the only complete sample of contact binaries with variability amplitudes >0.05 mag is that of the *Hipparcos* catalog (Rucinski 2002b), which extends to $V_{\max} = 7.5$. From now on we call this sample "the *Hipparcos* sample" or "the 7.5 mag sample." Beyond that limit, the *Hipparcos* target selection was driven by lists existing in the early 1980s, so the *Hipparcos* catalog is incomplete.

The original 7.5 mag sample, as defined in Rucinski (2002b), consists of 32 stars; in this there are 13 genuine contact binaries (EW), 14 ellipsoidal variables of small amplitude (EL), and 5 binaries with unequally deep minima (EB). Since small-amplitude contact binaries are expected to dominate in numbers (Rucinski 2001), it is reasonable to consider the EL and the EW systems together. It is not obvious whether we should add to these the EB systems (Rucinski 2002b), but their number is relatively small. For the purpose of this paper we decided to include in the 7.5 mag sample three triple systems (V867 Ara, KR Com, and HT Vir) for which the contact binary is slightly, by less than 0.1 mag, fainter than $V_{\max} = 7.5$ but the total brightness beyond that limit led previously to their elimination from the sample. This is consistent with the "fuzzy" $V_{\max} = 10$ limit that we adopt in this paper, as described below.

Assuming a simple scaling law for the uniform, homogeneous stellar density, we can expect that the 10 mag sample should be $\simeq$32 times larger than the 7.5 mag sample. Thus, it should have about 1000 binaries. In fact, the 10 mag sample consists of 151 objects, which directly shows that huge numbers of contact binaries still remain to be discovered in the interval $7.5 < V_{\max} < 10$. A part of this discrepancy is probably due to the detection threshold for variability amplitudes, which is about 0.05 mag for the *Hipparcos* sample but is not uniform and is possibly at a level of 0.1–0.2 mag for the 10 mag sample.

The 35 binaries in the *Hipparcos* sample are too few for meaningful statistical inferences, but it can provide some guidance on the incidence of triple systems for the $V_{\max} = 10$ sample. Utilizing techniques identical to those described in detail in this paper, we see 17 triple systems, which corresponds to the lower limit on the relative incidence of triple systems of $48\% \pm 12\%$. As we see in §§ 6 and 7, this is consistent with, but slightly lower than, the results for the full $V_{\max} = 10$ mag sample, indicating this fraction to be $59\% \pm 8\%$. We note that a large fraction of the *Hipparcos* sample (about one-third) is actually low photometric amplitude binaries discovered by this satellite; these binaries have been studied only during the last 7–8 yr and still have incomplete data.

We note that we encountered several difficulties in observing the strict limit of 10 mag. In particular, our definition of $V_{\max}$ refers to the combined magnitude of all components in the system, irrespective of whether this is just a binary or has a companion. Since we a priori do not know how many stars are in the system, such a "fuzzy" definition explicitly depends on the number of components in the system. While we recognize this uncertainty, we note that a comparable uncertainty of a few times 0.1 mag in the magnitude limit is currently introduced by differences between photometric systems and a generally poor state of uniform, calibrated photometric data for contact binaries. In the practical implementation of the $V_{\max} = 10$ limit we have been forced to use several sources. We usually took $V_{\max}$ from the General Catalogue of Variable Stars (GCVS).[1] For stars without $V_{\max}$ magnitudes in the GCVS, we used the 5th percentile of the *Hipparcos* brightness (field H49 in the *Hipparcos* catalog; Perryman et al. 1997); these H_p magnitudes were then transformed to Johnson photometric systems by interpolating in the tables of $H_p - V_J$ (Tables 1.3.5 and 1.3.6 in Vol. 1 of the *Hipparcos* catalog). For a few stars not observed during the *Hipparcos* mission and having only photographic or photovisual maximum magnitude in the GCVS, we took approximate $V_{\max}$ values from the original papers.

Finally, we note that we resisted very hard a temptation to use other samples in addition to the 10 mag sample. Some sources provided deeper samples. For example, a sample based on the *Hipparcos* astrometric data would consist of 177 systems and for some binaries would go well beyond the adopted magnitude limit. On the other hand, the *Hipparcos* sample is incomplete before the 10 mag limit is reached, and some bright systems are not included or have poor data. Other techniques and methods that we used had different biases and limitations, so that we would have to analyze each sample separately. In the end, we decided to strictly observe the limit of $V_{\max} = 10$, which results in the final sample of 151 binaries. We list binaries fainter than 10 mag separately in the second half of Table 1, but we do not utilize them for the multiplicity frequency estimates or show them in frequency plots. They are included here partly for the record, with an expectation that the magnitude limit will soon be improved, and partly to show that different techniques and multiplicity indicators have different properties at faint brightness levels. We note that Table 1 may be taken as a useful list for further work on candidates for multiplicity.

3. DIRECT IMAGING AND ASTROMETRY

3.1. *The WDS Catalog and Hipparcos Data* (*Flag 1*)

The most obvious of all detection techniques is direct visual detection using speckle interferometry or high-resolution imaging (see, e.g., Hershey 1975). A large body of data for multiple stars has been collected by Tokovinin (1997, 2004); his comprehensive Catalogue of Physical Multiple Stars provides data on such quantities as the brightness, distance, position angle, astrometric data, and hierarchy in multiple systems. These data have been used in the present study together with the *Hipparcos* catalog (Perryman et al. 1997) data, augmented by the post-*Hipparcos* improved orbits of many wide systems by Söderhjelm (1999), with component separation and photometric data revised by Fabricius & Makarov (2000).

A visual detection should involve confirmation of the physical link, which is usually relatively simple for contact binaries, as, photometrically, they occur within the width of the MS, so a plausible combination of magnitude and color differences is usually sufficient to establish a physical connection. The main problem

[1] Available at http://www.sai.msu.su/groups/cluster/gcvs; we used the most recent electronic version, 4.2.

here is the lack of standardized photometric data for a large fraction of contact systems. Bright, and hence nearby, contact binaries appear randomly on the sky, usually on an empty sky so that the presence of a close visual companion can frequently be taken as an indication of triplicity, which obviously requires confirmation.

Visual detections and astrometric data have been accumulated over a long time as a result of many investigations using different instruments and methods. The Washington Double Star Catalog (WDS; Mason et al. 2001b) appears to be the most complete and best-updated compilation of these results; the major contributor to the WDS is the *Hipparcos* satellite mission (Perryman et al. 1997). One of great contributions of this satellite, in addition to the well-known astrometric results, was in the photometric discovery of many low-amplitude, 0.05 mag $< \Delta V <$ 0.2 mag, variables. Inclusion of these variables dramatically improved the available data on the statistics of close binaries (Rucinski 2002b) after appropriate allowance for binaries misclassified as pulsating variables, particularly after a major effort to identify those unrecognized contact binaries by Duerbeck (1997).

Among the 137 systems listed in the *Hipparcos* catalog, 43 are listed in the WDS as forming visual binaries with a distant third body, although some (e.g., AW UMa; see § 6) are in proper-motion pairs with very long, practically unmeasurable orbital periods, yet at physical separations indicating a common origin. The multiplicity of a few systems (V867 Ara, QW Gem, CN Hyi, V1387 Ori, Y Sex, and TU UMi) was discovered by the *Hipparcos* mission, while the multiplicity of CV Cyg and EF Dra was discovered by the Tycho project of that mission (see the Tycho Double-Star Catalogue; Fabricius et al. 2002).

In order to avoid a distance bias, instead of the angular sky separation (ρ) as a criterion of a physical link we used distances to find the projected separations in AU. For systems having *Hipparcos* parallaxes (π) with a relative error less than 20%, the separations were determined as ρ/π. Distances to systems without reliable parallaxes were determined using the absolute magnitude calibration of Rucinski & Duerbeck (1997), which is based on the orbital period and color index; for a few systems, the color index had to be estimated from the spectral type or even more crudely from the orbital period. For EM Cep and V395 And the $(B - V)$ index is too blue for the calibration to apply. For EM Cep a distance of $d = 794$ pc was adopted, assuming its membership in NGC 7160 (Kharchenko et al. 2005). The spectral type of B7–8 for V395 And with the MS components implies a distance of 450 pc, but this is an upper limit, as the components can be sdB stars (Rucinski et al. 2005).

The direct visual detections documented in the WDS are marked in Table 1 by the first of the eight flags (Flag 1), which can take the following designations: "D" for detected (separations less than 2000 AU or 0.01 pc), "P" for possible cases (separations between 2000 and 20,000 AU, corresponding to 0.01–0.1 pc), and "N" for separations larger than 20,000 AU.

3.2. *Adaptive Optics CFHT Program* (*Flag 2*)

A program of direct detection of infrared companions using the adaptive optics system on the Canada-France-Hawaii Telescope (CFHT) was undertaken by one of the authors (S. M. R.) on two nights in 1998. It consisted of one-color, one-epoch, high spatial resolution imaging to $<0''.1$. The data have been analyzed in a cursory way because continuation of the program is expected, so the results should be considered as preliminary.

The observations were obtained with the PUEO instrument and the KIR camera combination (Rigaut et al. 1998) in the H and K infrared bands (1.65 and 2.2 μm) on 1998 January 10/11 and July 23/24. Most observations were done in the K band and its narrowband version, the K_{CO} band, with a few binaries also observed in the H band. Fields of $36'' \times 36''$ were observed, centered on contact binaries visible from CFHT to approximately $V < 10.5$. The scale on the detector was $0''.0348$ pixel^{-1}. The measured FWHM of corrected images was $0''.143$ in the K band, which is very close to the expected diffraction-limited performance of a 3.6 m telescope. We used point-spread function subtraction only for obvious, easily visible companions at separations below $1''$; we did not apply this technique to search for new, faint companions perhaps hiding in the diffraction ring structure of the primary—this may be attempted in the future. In spite of the cursory treatment, we detected seven previously unidentified companions at separations smaller than $5''$ to GZ And, AH Aur, CK Boo, SW Lac, V508 Oph, U Peg, and RZ Tau. In all those cases, judging by the values of magnitude differences ΔK and ΔH we suspect the companions to be late-type dwarfs. We estimate that our detection limit in the sense of the smallest separations is about $0''.08$ (for a system with identical components); this is based on the case of CK Boo, where a fainter companion was easy to detect at a separation of $0''.12$.

Some of the observed fields contain close companions at moderate angular separations ($5'' \leq \rho \leq 25''$), which may be physically associated with the central contact binaries because such angular separations for nearby stars still imply physical distances between stars well below the typical average in the solar neighborhood. These cases must be supported by other evidence that we currently do not have. Results of the CFHT observations are listed in Table 4. We give the separation in arcseconds, the position angle in degrees, and the difference in magnitudes relative to the primary (contact binary) component in the K or H bands. The final assessment of the physical connection is based—similar to that for the directly observable visual binaries (§ 3.1)—on the projected separation of the components. In Table 1 the results are coded by Flag 2, similar to those for objects discussed in § 3.1, except for the symbol "–," which signifies that the star was not observed.

3.3. *Detection through Astrometric Solutions* (*Flag 3*)

The most important astrometric results and the reason for the *Hipparcos* mission were trigonometric parallaxes of nearby stars. Parallax errors and quality estimates of astrometric and orbital solutions are cataloged in the *Hipparcos* Double and Multiple Annex for all known or discovered visual pairs. We present here an argument that the parallax error data carry useful information on multiplicity.

The *Hipparcos* parallax error depends primarily on the brightness and less so on the ecliptic latitude of a system, but it increases if an unseen component causes a transverse motion of the star on the sky. The astrometric solution can also be deteriorated by a variability-induced motion of the photocenter in a close visual or unresolved system with a variable component; such a motion can be particularly pronounced for large-amplitude variables such as Mira pulsating stars (Pourbaix et al. 2003) but may also affect all other variables, including contact binaries. In what follows we analyze the parallax errors as indicators of multiplicity of contact binaries.[2] For an assessment of the multiplicity, the most important *Hipparcos* catalog data are as follows:

1. The astrometric solution type (catalog field code H59), the first character in the column headed "HIP" in Table 1.[3] It takes

[2] One of the notable multiple systems without a parallax is GZ And. Together with a few similar stars close by in the sky, it appears to form a genuine multiple-star trapezium configuration (Walker 1973).

[3] Two other *Hipparcos* H59 flags do not occur within our sample: "O" for astrometric orbital solution and "V" for variability induced motion; also, a "D" type of visual solution has never occurred.

TABLE 4

CFHT Adaptive Optics Observations (1998)

Name[a]	Component	ρ (arcsec)	θ (deg)	ΔK	ΔH	HJD−2,450,800	Flag	Comments
Binaries Brighter than $V = 10$								
AB And		18.9	306	7.3		219.04	P	Uncertain
GZ And[b]	B	8.6	36	−0.2	−0.3	219.10	D	Poor seeing
GZ And[b]	C	13.3	196	−0.3	0.0	219.10		Poor seeing
GZ And[b,*]	E	2.13	33	2.4	2.6	219.10		Poor seeing
GZ And[b,*]	F	13.3	134	5.0	5.5	219.10		Poor seeing
CK Boo*		0.12	196	2.8		218.80	D	
SX Crv						218.75	N	
V1073 Cyg						218.98	N	Poor seeing
YY Eri						24.79	N	
BV Eri						219.12	N	
AK Her		4.5	324	2.0		218.88	D	Poor seeing
FG Hya		16.5	145	4.0		24.96	P	
SW Lac*		1.68	85	2.5	2.6	219.02	D	
UZ Leo						25.05	N	Poor observation
XY Leo						25.01	N	
AP Leo						25.07	N	
UV Lyn						24.99	N	
V502 Oph						218.87	N	Poor seeing
V566 Oph						218.89	N	Poor seeing
V839 Oph		8.2	8	6.1		218.92	D	Poor seeing
V839 Oph		22.3	36	2.7		218.92		Poor seeing
ER Ori[c]	C	0.17	353	2.2		24.85	D	
ER Ori[c]	B	14.4	10	2.6		24.85		
U Peg*		4.05	275	5.2		219.07	D	
AQ Psc		21.5	33	4.2		24.71	P	
AQ Psc		21.5	33	3.4		219.08		
AQ Psc		25.8	65	3.5		24.72		
AQ Psc		25.8	65	3.0		219.08		
TY Pup		8.4	2	3.8		24.93	P	
V781 Tau		30.0	318	3.0		24.88	D	
V781 Tau		14.6	163	8.0		24.88		Uncertain
AG Vir						25.09	N	
AH Vir		1.71	17	1.6		25.11	D	
GR Vir						218.82	N	
Binaries Fainter than $V = 10$								
AH Aur*		3.18	63	4.2	4.0	24.90	D	
AH Aur		17.2	80	7.1	7.1	24.90		Uncertain
AH Aur		21.8	326	6.6	6.6	24.90		Uncertain
TZ Boo		10.6	120	6.9		218.84	D	Uncertain
RW Com						25.12	N	Poor observation
DK Cyg						218.99	N	Poor seeing
V401 Cyg		18.0	359	1.2		218.93	P	Poor seeing
UX Eri						24.76	N	Poor observation
XZ Leo		18.3	112	7.0		25.03	P	Uncertain
VZ Lib						218.86	N	Poor seeing
V508 Oph*		2.40	19	3.9	4.2	218.90	D	Poor seeing
V508 Oph		13.9	192	4.6	4.8	218.90		Poor seeing
BB Peg						219.01	N	
RZ Tau*		0.80	43	3.7		24.81	D	
RZ Tau*		0.80	44	3.9		219.13		

Notes.—Comments on poor observations: poor seeing, the AO system worked poorly when the natural seeing was worse than 1″; poor observation, the central star (contact binary) is saturated in some images; uncertain, the detected companion was very faint, at the limit of detection. Here ΔK- and ΔH-magnitude differences relative to the central (contact binary) star were measured with accuracy of about 0.1–0.2 mag. The column headed "Flag" gives our rating of the target, corresponding to that in Table 1. The flag is given only in the line of first appearance of the target.

[a] The asterisks (*) denote new detections at separations $<5''$.

[b] GZ And: Components B and C, as identified in Walker (1973). Component D was outside the field of view. Components E and F are new.

[c] ER Ori: The more distant companion known before is called B, while the physical companion discovered by Goecking et al. (1994) and confirmed here is called C.

values of "C" for a linear motion of components, "X" for a stochastic solution, and "G" for an acceleration term being necessary. While "X" and "G" apply for apparently single stars (six cases in our sample),[4] "C" refers to known visual systems.

2. The quality of the double or multiple star solution (field code H61). This is indicated by the second symbol in the column headed "HIP" in Table 1. The flag "S" indicates that a possible, although unconvincing, nonsingle solution was found for an apparently single star; 17 such systems appear in our sample. For known visual binaries, the solutions are coded "A" to "D," in progression from best to worst. A very poor quality solution (i.e., the flags "C" or "D") indicates a possible additional perturbation in the visual system.

3. The *Hipparcos* parallax error (field H16), indicated by the column headed "σ_π" in Table 1. Thirty-five systems have parallax errors more than 3 σ larger than the respective median values at given brightness levels.

An inspection of the catalog shows that three contact systems, V353 Peg, ER Ori, and V2388 Oph, required an acceleration term in the astrometric solution, and hence, they are most probably astrometric double stars with orbital periods longer than about 10 yr (see § 2.3.3 of the *Hipparcos* catalog). The acceleration terms in the astrometric solution of ER Ori are relatively large: $g_\alpha = -19.26 \pm 6.57$ mas yr^{-2} and $g_\delta = -17.34 \pm 4.71$ mas yr^{-2} (the unit "mas" is equal to 0.″001, a milliarcsecond). Several systems, which are very probably unresolved visual binaries, show "stochastic" scatter, i.e., an excessive random scatter in deviations from their astrometric solutions (CL Cet, BE Scl, FI Boo, AK Her, V401 Cyg, and CW Sge).[5] The so-called cosmic error ϵ given in the *Hipparcos* catalog describes the scatter in the astrometric solution. It is of considerable astrophysical interest, as it gives the most probable size of the astrometric orbit and points at relatively tight orbits with periods shorter than 1 yr. The cosmic error is largest for V401 Cyg with $\epsilon = 26.82 \pm 2.24$ mas and BE Scl with $\epsilon = 13.36 \pm 1.35$ mas. The systems are prime candidates for speckle interferometric observations. In fact, Mason et al. (1999, 2001a) performed speckle interferometry of *Hipparcos* doubles and *Hipparcos* problem stars (i.e., stars having "V," "O," "G," or "X" in H59 or "S" in H61) and detected 15 new visual doubles with a mean separation of about 0.″2. Among these stars was V353 Peg ("G" flag in H59), but no companion of this star at an angular separation larger than 0.″035 was detected (Mason et al. 2001a).

The parallax error versus *Hipparcos* magnitude H_p is plotted in Figure 1. The figure clearly shows that known visual binaries (*filled circles*) show large parallax errors, a condition that can be used as a criterion indicating multiplicity. The large parallax errors also correspond to stochastic solutions or to cases in which a necessity of acceleration term occurred (*squares*). Of note is the case of ER Ori, which has a formally *negative* parallax $\pi = -6.68$ mas. In addition to the systems already indicated in the *Hipparcos* catalog, the large parallax errors of DY Cet, UX Eri, and V1363 Ori strongly suggest multiplicity.

A summary of all multiplicity indications derived from the astrometric parallax data appears in Table 1 under Flag 3. Detections are marked by "D" for "X" or "G" type solutions, while the suspected cases "S" correspond to those already suspected in the *Hipparcos* catalog ("S" in H61), systems with "C" type

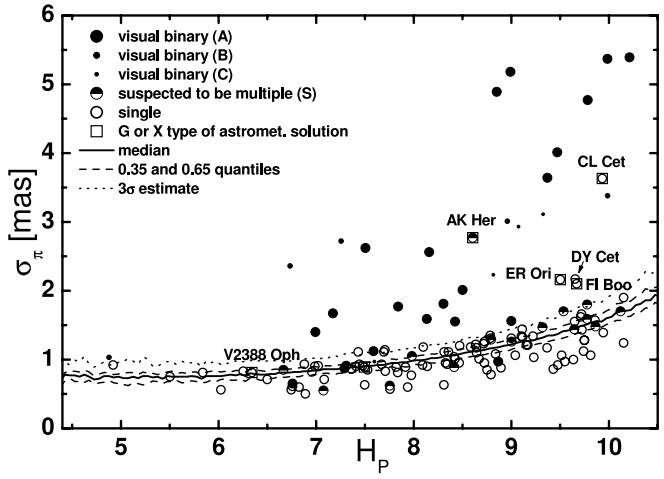

FIG. 1.—Parallax error vs. median H_p magnitude for contact binaries (*circles*). The same dependence for single stars in the *Hipparcos* catalog is shown by the solid line (labeled "median") in the lower part of the figure, with the corresponding statistical uncertainty ± 1 σ limits (labeled "0.35 and 0.65 quantiles") given by the dashed lines and the positive 3 σ range given by the dotted line. The known visual multiple systems among contact binaries are marked by filled circles, with their sizes indicating the quality of the astrometric solutions, as given in the catalog H61 field (A, "good"; B, "fair"; C, "poor"). Binaries with "G" or "X" type astrometric solutions (see the text) have squares around them. We argue that binaries above the curve are strongly suspected to belong to multiple systems.

quality of orbital solutions,[6] and systems with parallax errors more than 3 σ from the median error (where σ is the rms uncertainty in the median error value). Three systems not recognized before as "S" cases, but having parallax errors larger than 3 σ relative to the error median, have been added here: UX Eri, V1363 Eri, and DY Cet. Here "N" signifies no detection. If a system was not included in the *Hipparcos* missions, then Flag 3 is "–."

In terms of its precision, the *Hipparcos* sample is biased mainly by two factors, the apparent brightness and the distance, as astrometric effects are smaller at larger distances. As a partial result on the true frequency of triple systems, and to visualize potential biases, we attempted to estimate the fraction of visual and astrometric triples solely from the astrometric data for the nearest, best-observed contact binaries. For this, we ranked the binaries according to the parallax, with the system of rank 1 being the closest contact binary 44 Boo. This sample contains 133 contact binaries brighter than $V_{\max} = 10$ that appear in the *Hipparcos* catalog and have positive astrometric parallaxes. In Figure 2 the left vertical axis gives the fraction of systems below and including a given rank, listed as visual binaries in WDS and suspected in *Hipparcos* (flags "X," "G," and "S"). The right vertical axis gives the total number of such systems for the given rank. Since one of the visual components is a contact binary, these systems are at least triple. For the 50 closest contact systems, the fraction of systems being at least triple shows a plateau and appears to be 40%, although the Poissonian noise at that point is about 9%. Such an estimate of the triple-system frequency, based only on the astrometric data, is incomplete, as we have direct evidence that the true frequency is higher: an additional eight multiple systems with contact binaries were detected spectroscopically (§ 4) without any astrometric indications of multiplicity (not even the "S" flag) in the *Hipparcos* astrometric data, while two more very close systems (CK Boo and U Peg) were discovered during the CFHT adaptive optics observations (§ 3.2).

[4] By a "single" star in this context, we mean a contact binary without additional components directly resolved on the sky. Visual binaries with one component being a contact binary are therefore, strictly speaking, triple systems.

[5] Note that V401 Cyg, CW Sge, and BE Scl, as well as UX Eri and V1363 Ori, are slightly fainter than 10 mag and thus appear in the second half of Table 1.

[6] This code may indicate an additional disturbance in the orbital solution and a higher multiplicity.

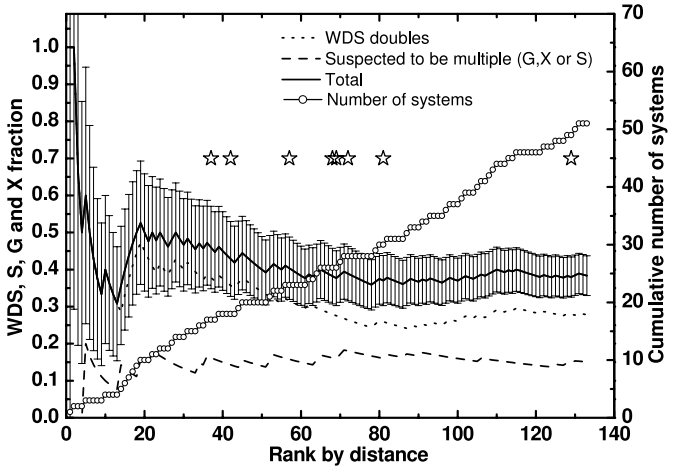

FIG. 2.—Fraction of visual double systems among the *Hipparcos* contact binaries, ranked by increasing distance of the sample to $V_{max} = 10$. The fractions for systems suspected of being double stars ("S" flag in the field H61) or showing an acceleration term or a stochastic solution ("G" and "X" flags in H59) are also given. The number of systems to a given rank is shown by the circles connected by a rising line, with the scale on the right axis. The stars mark ranks of triple systems detected spectroscopically but without any indication of multiplicity in the astrometric data; this visualizes the need for the independent application of spectroscopy for a complete picture. Error bars represent estimated Poissonian errors. They were computed as the square root of the number of systems below and including the given rank.

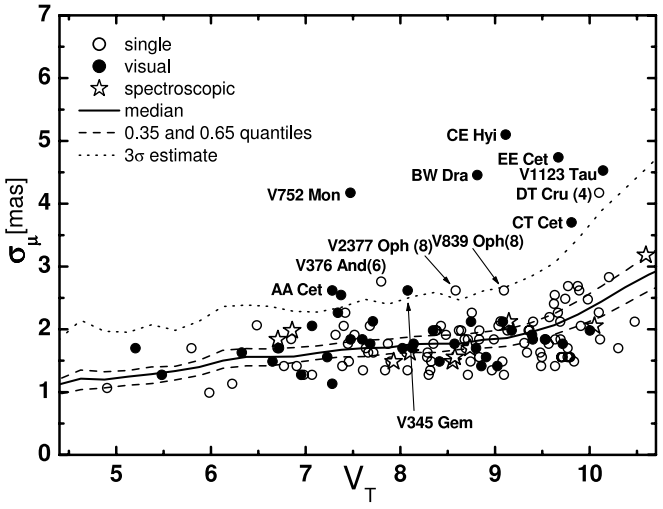

FIG. 3.—Dependence of the combined proper-motion error, σ_μ, on the median V_T magnitude for all contact binaries in the Tycho-2 catalog. This figure is analogous to Fig. 1, and the lines here have the same meaning as there. All contact binaries are marked by circles, with those in known visual binaries marked by filled circles. Numbers written in parentheses are given for systems currently not identified as multiple systems but with a small number of astrometric observations available for proper-motion determination; these cases should be treated with considerable caution. The stars mark spectroscopic binaries; it should be noted that none would be detected by the proper-motion error technique.

3.4. *Proper-Motion Errors* (*Flag 4*)

The *Hipparcos* mission provided an excellent new epoch datum for proper-motion studies of nearby stars. Proper-motion data improve over time as the time base grows. Use of the old data led to the main improvement in the proper-motion results from the Tycho-2 project (Høg et al. 2000) when compared with the original *Hipparcos* results based on 3 yr of satellite operation. We can use this material the same way as described above for the parallax errors by analyzing individual errors of the proper-motion determinations.

We note that the proper-motion errors depend on many factors, such as (1) the time interval covered by observations, (2) the number and quality of astrometric data, and (3) the brightness of the system. Figure 3 presents evidence that known visual systems among contact binaries have larger proper-motion errors, so that the situation is indeed analogous to that with the parallax errors. The difference is in the timescale of the external orbit, as this indicator is sensitive to companions orbiting on large orbits, with the Tycho-2 data sensitive to periods spanning perhaps as long as a fraction of a century; this should be contrasted with the *Hipparcos* parallax errors, which were estimated from internal uncertainties of the mission lasting 3 yr.

In Figure 3, note the known members of visual binaries such as EE Cet or V752 Mon. Other systems, like V376 And or V2377 Oph, may be members of triple systems with relatively long-period orbits. For the statistics in Table 1, we treat as suspicious cases all systems with proper-motion errors 3 σ above the Tycho-2 error median, as before assuming σ to be the rms uncertainty of the median. We include FU Dra, V829 Her, and V839 Oph, which are close to this limit. We note that in the error estimation, one must be careful with systems having only three astrometric observations, as one erroneous observation would result in a large error of the derived proper motion.

4. SPECTROSCOPY (FLAG 5)

4.1. *Line Profiles and Broadening Functions*

Spectroscopy offers one of the most direct methods for the discovery of companions to contact binaries. When a companion is present, extraction techniques using the deconvolution of spectra, such as the broadening functions (BFs; see Rucinski 2002a) or their poor-quality substitute, the cross-correlation function, often show one sharp peak superposed on a background of a broad and rapidly changing projection of the contact binary brightness onto the radial velocity space.

The radial velocity program at DDO (currently at Paper X and 90th orbit; Rucinski et al. 2005) is specifically designed to provide radial velocity data for close binary systems with periods shorter than 1 day and brighter than about 10 mag. It was noticed almost from the beginning of the program in 1999 that our sample contained many triple systems with third components frequently dominating in light. This turned out not to be an accidental occurrence but an interesting, if mild, bias in our sample: our candidates have been predominantly from among recent photometric discoveries—frequently by the *Hipparcos* project—with small photometric amplitudes. While for some of these cases the low amplitudes happened to be due to a low orbital inclination, for many binaries, when a companion is present, the reason is the "dilution" of the photometric signal in the combined light. These low photometric amplitude binaries were not known until the systematic (to $V \simeq 7.5$) *Hipparcos* survey took place. Spectroscopically, these stars had been frequently overlooked as their spectra—even when the companion is relatively fainter—typically show only one sharp-line component, sometimes only with some fine and hard-to-detect continuum peculiarities (Rucinski 2002a).

At this time, out of 90 stars with new, reliable elements determined during the DDO spectroscopic binary program, 76 are contact binaries or probable contact binaries. Among these, 12 are members of visual binaries, some already identified by other techniques. We discovered spectroscopic companions in V899 Her and VZ Lib (Lu et al. 2001), V401 Cyg (Rucinski et al. 2002), and VW LMi, TV UMi, and AG Vir (Pribulla et al. 2006). But not all of our detections were new: because of the moderately poor seeing at the DDO site with a median FWHM of about 1.″8, some already known astrometric companions were not visible directly

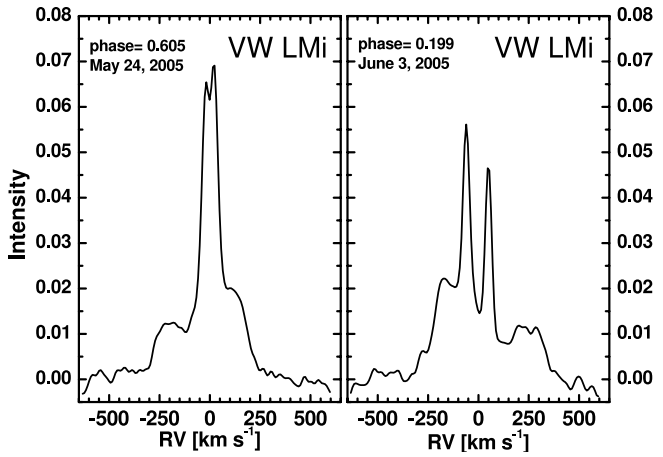

FIG. 4.—BFs of the quadruple system VW LMi extracted from spectra taken on 2005 May 24 (*left*) and June 3 (*right*). The contact binary signature is in the strongly broadened profiles, while the profiles for the slowly rotating components of the second, long-period, detached binary are narrow. Splitting of the lines of the detached pair occurs only on a few days around the periastron passage.

during the observations and appeared for the first time in the spectroscopically derived BFs. This way, we rediscovered several multiple systems (e.g., EF Dra and V410 Aur). Examples of the BFs for the spectroscopically triple systems can be found in the series of DDO publications, particularly in Paper IV (Lu et al. 2001), Paper VI (Rucinski et al. 2002), and Paper VIII (Rucinski et al. 2003). Here we show in Figure 4 the BFs for an even more complex quadruple system, VW LMi, whose complicated nature has been discovered during the DDO program (Pribulla et al. 2006).

The detection limit for spectroscopic companions, given by the ratio of the third-component light to the total light of the eclipsing pair $\beta = l_3/(l_1 + l_2)$, at our spectral window at 5184 Å is about 0.03–0.04. This estimate is based on the cases of V401 Cyg ($\beta = 0.03$) and HX UMa ($\beta = 0.05$), in which a weak light contribution was easily detectable. This corresponds to $\Delta m \simeq 3.8$ in the most favorable case; normally, the detection limit depends on the shape of the combined BF, as the sharp peak may sometimes hide within the two lobes of the binary. An opposite extreme case of a bright companion entirely masking any traces of the contact binary in the broadening function is V752 Mon (new, unpublished DDO observations), for which at $\Delta m \simeq -0.5$ the companion is a rapidly rotating A-type star with $V \sin i \sim 220$ km s^{-1}. Generally, it is difficult to map the domain of detection of third components, as it depends not only on β but also on the $(K_1 + K_2) \sin i$ value of the binary, its mass ratio, the $V \sin i$ value of the third component, etc.

4.2. *Composite Spectra*

While our individual BFs used for radial velocity measurements have a limitation for the smallest β detectable at a given signal-to-noise ratio, averaging of the same spectra may show fainter companions to $\beta \simeq 0.01$ or even below. While the binary signatures are smeared out through averaging, any constant component gains in definition. This is exactly the approach taken in Paper II, where spectra previously used in the DDO radial velocity have been used to detect weak TiO features of M-type dwarfs in, e.g., SW Lac, CK Boo, and BB Peg. A particularly good example is SW Lac, which was not seen in individual BFs (Rucinski et al. 2005) but could be convincingly detected in the average spectrum. The faint companions are also detectable through the presence of the molecular bands of TiO, VO, and CaH. In the visual and near-infrared regions, the TiO bands are the dominant source of molecular absorption in stars later than M3 (see Kirkpatrick et al. 1991). Particularly prominent TiO features occur at around 5500 and around 7600 Å.

We refer to Paper II for details of the spectrum-averaging technique, which is discussed there with a particular stress on its biases and limitations. The spectral region used at DDO for the radial velocity program, of about 200–300 Å (depending on the CCD detector) centered at 5184 Å, is a very convenient one for radial velocity measurements because the magnesium triplet "*b*" feature is strong over a wide range of spectral types from middle A to early K types but is not optimal for the detection of faint, low-temperature companions. For that reason, we plan to conduct a search based on good quality, low-dispersion, red spectra of contact binaries with a specific goal of detecting molecular features characteristic of late-type companions.

We note that the disentangling technique (Hadrava 2004) has the potential to determine the individual spectra from multicomponent spectra undergoing radial velocity shifts. The method produces orbital parameters of the spectroscopic binary, as well as information on any additional spectrum in the system; thus, telluric lines, as well as lines of a third component, are naturally determined.

Flag 5 in Table 1 gives information on triplicity as determined from spectroscopy, both in the radial velocity program and in the averaged spectral data. The codes used are "D" for detection, "S" for suspicion, "N" for not detected, and "–" for not yet observed or not analyzed.

4.3. *Systemic Velocity Changes*

A scatter or trends in the center-of-mass velocity, V_0, may indicate the presence of companions. Because radial velocities usually come from different sources with different systematic errors and because contact binaries show a large broadening of spectral lines, this is a difficult to apply and generally poor indicator of multiplicity. As we see below, the required accuracy for V_0 (i.e., precision combined with systematic uncertainties) for the well-known close visual multiple systems of 44 Boo and VW Cep is at a level of 1 km s^{-1}, which is very difficult to obtain for contact binaries. To complicate things, very few contact binaries have been observed for radial velocities at more than one epoch so that a comparison of published systemic velocities can be done for only a few objects:

1. AB And has three sets of spectroscopic elements (Struve et al. 1950; Hrivnak 1988; Pych et al. 2004). While the second and the third sources give similar V_0, the first gives a velocity shifted by -16 km s^{-1}.

2. 44 Boo has several RV studies. The results of early studies are discussed by Hill et al. (1989), with the most reliable data subsequently published by Lu et al. (2001). Systemic velocity changes were observed to range between +3.9 and -32 km s^{-1}, which is much more than the expected full amplitude for the well-studied visual system of only 0.7 km s^{-1}. We suspect that the scatter in V_0 is purely instrumental in this case.

3. VW Cep was observed five times; see Pribulla et al. (2000) for the discussion and references. The systemic velocity shows a much larger spread (-35 to +10 km s^{-1}) than can be expected from the known third body, expected to cause a full amplitude of $\approx$5.8 km s^{-1}. Again, the most likely reason for the scatter is instrumental.

4. Spectral lines of a third component were detected in SW Lac by Hendry & Mochnacki (1998). Three available systemic velocities (Struve 1949; Zhai & Lu 1989; Rucinski et al. 2005) range

between -15 and -10 km s^{-1}, which can be considered as a case of exceptionally good agreement and thus constancy of the mean velocity. This is somewhat paradoxical, as we know that the system contains at least one additional component.

5. V502 Oph has had four studies (Struve & Gratton 1948; Struve & Zebergs 1959; King & Hilditch 1984; Pych et al. 2004). Struve & Zebergs (1959) noted a -13 km s^{-1} shift in radial velocities between their two runs. Lines of a third component were detected by Hendry & Mochnacki (1998).

6. There exist seven published radial velocity data sets for W UMa (Rucinski et al. 1993). Systemic velocities show large variability in the range from -43 to 0 km s^{-1}. Part of the scatter can be instrumental, but the presence of a third body in the system is possible.

7. The possible multiplicity of AW UMa has been discussed in Pribulla et al. (1999b). The observed systemic velocity changes would require a relatively massive body, which was not detected in BFs of the system (Rucinski 1992). The system is a prime candidate for a new spectroscopic study.

On the basis of the observed large systemic velocity changes, two systems, W UMa and AW UMa, are coded as "S" (suspected) in Flag 5 in Table 1.

5. INDIRECT MULTIPLICITY INDICATORS

5.1. *The Light-Time Effect* (*Flag 6*)

Accelerated or delayed times of eclipses in close binaries are normally interpreted as a result of apparent period changes. These changes may result from the binary revolution on a wide orbit around a center of mass with a companion; this is then frequently called the light-time effect (LITE; Borkovits & Hegedus 1996). Because intrinsic period changes in close binaries are quite common due to their strong physical interaction, the presence of the LITE is usually not conclusive, but it can prompt other observations. Such was the case for VW Cep, where periodic variation of the eclipse times was interpreted by the LITE very early by Payne-Gaposhkin (1941). In 1974 the third component was indicated by the transverse motion of the contact pair and then was directly observed (Hershey 1975).

The period of an eclipsing binary is the most precisely determined orbital element due to the accumulation of period deviations over many orbits. Traditionally, timing of eclipses has been a separate activity concentrated on the light minima only (Kreiner et al. 2001), but new techniques use whole light curves (Genet & Smith 2004), while new light-curve-fitting codes even include the LITE to enable the analysis of short-period triple systems (W. van Hamme 2005, private communication).

The LITE technique has several advantages over the other approaches because (1) it is distance-independent, (2) light minima can be observed with small telescopes, (3) the time delay/advance effect, in contrast to its spectroscopic amplitude counterpart (the variation in V_0), increases with the period of the third body, and (4) detection is independent of the relative brightness of the third component. The technique also has pitfalls: (1) The behavior of $O-C$ residuals (observed minus calculated time of eclipse) very often indicates periods similar to about two-thirds of the used time interval; this may be a signal of a failure in the main LITE assumptions leading to overinterpretation of the data. (2) Detection of short-period orbits may be negatively influenced by the enhanced surface activity (Pribulla et al. 2005), and migrating spots can sometimes cause wavelike behavior of the $O-C$ diagrams (see, e.g., Kalimeris et al. 2002); fortunately, the spot-induced shifts of the eclipse minima usually only increase the scatter of observed minima times (Pribulla et al. 2001). (3) Another possible interpretation of the cyclic period changes is a periodic transfer of the orbital angular momentum to magnetic momentum in active systems (Applegate 1992); while this may be the case, the actual confirmation of this mechanism still remains to be done and is still controversial (Pribulla et al. 2001; Afsar et al. 2004).

The formulae for the theoretical LITE computation can be found in Irwin (1959). An observed time of the minimum light can be predicted as follows:

$$\mathrm{JD(Min.\ I)} = \mathrm{JD}_0 + PE + QE^2 + \frac{a_{12}\sin i}{c}\left[\frac{1-e^2}{1+e\cos\nu}\sin(\nu+\omega) + e\sin\omega\right], \quad (1)$$

where c is the speed of light; $\mathrm{JD}_0 + PE + QE^2$ is the quadratic ephemeris of the eclipsing pair (a secular change of the period measured by Q is the most likely type of change for the binary itself); a_{12}, i, e, and ω are the orbital parameters; and ν is the true anomaly of the binary on the orbit around the common center of gravity with the third body. Since the LITE operates in the radial direction through a mechanism similar to the Doppler effect, the LITE parameters are similar to spectroscopic elements. The problem of cyclic variations in the period is one of a simple model fitting: given pairs JD(Min. I) and E, one must optimize the parameters P_3, $a_{12}\sin i$, ω, e, and T_0 and the ephemeris of the eclipsing pair JD_0, P, Q.

For the present analysis, the contact binaries were selected from the updated version of the Catalogue of Contact Binary Stars (CCBS; Pribulla et al. 2003), currently containing 391 systems. Among these, 129 have more than 15 CCD or photoelectric photometry (*pe*) minima in the Cracow database (the 2004 May version; Kreiner et al. 2001). Because standard errors are available for only a small portion of the minima times and cannot be trusted, we applied an arbitrary weighting scheme with the weights assigned as $w = 10$ to *pe*, $w = 5$ to CCD, $w = 3$ to visual and photographic, and $w = 1$ to "patrol" and single-epoch plate minima. The weight $w \leq 3$ minima were used only in cases for which no other minima were available. Only 18 out of 129 systems provided stable LITE solutions. In our sample of contact binaries brighter than $V_{\max} = 10$ there are 57 systems with a sufficient number of minima; among them 11 have feasible LITE solutions.

An analysis of all available minima and new LITE solutions are presented here for TY Boo, TZ Boo, CK Boo, GW Cep, UX Eri, V566 Oph, and BB Peg. The resulting parameters are given in Table 5, while Figure 5 illustrates two rather typical cases, TZ Boo and BB Peg. For SW Lac and CK Boo the orbital period P_3 is very uncertain, and its inclusion as an unknown in fact destabilized the solutions. In the case of UX Eri, the inclusion of the orbital eccentricity destabilizes the solution.

In addition to the approximate orbital elements, Table 5 gives the minimum mass of the third body determined from the mass function and total masses of the eclipsing pair. For the latter, we used the CCBS data, in available cases modified by values determined in the DDO program of spectroscopic orbit determinations (see Rucinski et al. 2005). We also give the expected angular separation of the third (or multiple) components in arcseconds for cases of available trigonometric parallaxes, evaluated as $\alpha = \pi a_{12}\sin i_3 (m_{12}+m_3)/m_3$.

Inspection of Table 5 shows that minimum masses for some systems (AH Vir, ER Ori, CK Boo, and the outer body in SW Lac) appear to be unrealistically high, which indicates that cyclic variations may have been caused by other effects, perhaps intrinsic to

TABLE 5

LITE Orbits, Estimated Masses, and Angular Distances of Multiple Components

Name	P_3 (yr)	e_3	$a_{12} \sin i$ (AU)	$f(m)$ ($M_\odot$)	Cycle	$M_{12} \sin^3 i$ ($M_\odot$)	i (deg)	M_{12} ($M_\odot$)	M_3 $i = 90^\circ$	π (mas)	α (mas)	ΔV_0 (km s^{-1})	A (days)	Flag	Reference
Binaries Brighter than $V = 10$															
AB And	59.1(10)	0.12(3)	3.77(6)	0.0153(9)	1.72	1.648	86.8	1.656	0.40	8.34	160	2.09	0.0433	D	1
BX And	62(9)	0.3(3)	2.2(3)	0.0027(11)	1.68		74.5			6.60		2.20	0.0254	S	2
CK Boo	21.3[f]	0.96(7):	5(4)	0.3(6)	1.36	1.171	56.6	2.012	1.50	6.38	300:	40:	0.0244	S	
VW Cep	27.8(2)	0.54(4)	2.28(6)	0.0153(12)	2.80	1.280	63.6	1.781	0.42	36.16	390	5.82	0.0246	D	3
AK Her	57.8(8)	0.16(6)	1.65(6)	0.00134(16)	1.81		80.8			10.47		1.72	0.0190	D	1
SW Lac3	93.1[f]	0.71(1)	15.2(2)	0.405(9)	1.27	2.101	80.2	2.196	1.89	12.30	400	13.82	0.1294	D	4
SW Lac4	28.2(1)	0.51(5)	2.58(9)	0.021(3)	4.20	2.101	80.2	2.196	0.54	12.30	160	6.33	0.0278	D	4
XY Leo	19.59(5)	0.09(3)	4.08(4)	0.1774(58)	3.01	1.046	65.8	1.378	1.00	15.86	140	12.36	0.0470	D	5
V566 Oph	23.1(5)	0.6(2)	1.2(2)	0.0031(17)	2.60	1.743	79.8	1.828	0.24	13.98	140	4.01	0.0111	D	
ER Ori	52(3)	0.77(5)	5.7(5)	0.068(18)	1.40	2.503	87.5	2.510	0.93	−6.68		12.69	0.0418	S	6
AW UMa	16.8(5)	0.46(22)	0.44(6)	0.00030(12)	2.33	1.815	78.3	1.933	0.11	15.13	120	1.77	0.0051	D	7
AH Vir	41.1(15)	0.89(5)	4.2(8)	0.042(24)	1.88	1.889	86.5	1.900	0.65	10.86	180	13.21	0.0219	D	8
Binaries Fainter than $V = 10$															
TY Boo	55.8(27)	0.26(7)	4.1(3)	0.0214(47)	1.38	1.637	77.5	1.759	0.47			4.48	0.0457	S	
TZ Boo	34.0(5)	0.58(4)	6.3(2)	0.217(23)	2.30	0.691				6.76		13.50	0.0708	D	
V523 Cas	86(5)	0.08(7)	4.8(4)	0.015(4)	1.17	1.110	83.8	1.130	0.31			3.35	0.0558	S	9
GW Cep	13.5(5)	0.58(28)	0.69(8)	0.0018(7)	3.06		84.0					3.72	0.0079	D	
UX Eri	42.8(13)	0.6[f]	3.9(3)	0.033(7)	1.74	1.798	79.0	1.901	0.59	6.57	110	6.80	0.0366	S	
V829 Her	10.9(6)	0.26(32)	0.9(2)	0.006(4)	1.37	1.062	57.0	1.800	0.30			5.16	0.0102	S	10
BB Peg	20.4(4)	0.32(21)	0.83(9)	0.0014(5)	3.59	1.862	79.9	1.951	0.19	3.02	30:	2.59	0.0092	S	
EQ Tau	50.2(18)	0.37(12)	3.9(4)	0.024(7)	1.22	1.749	86.6	1.752	0.49			5.21	0.0390	S	11

Notes.—Name: GCVS name. P_3: Orbital period of the third body in years. e_3: Orbital eccentricity. $a_{12} \sin i$: Semimajor axis of the eclipsing binary orbit around the common center of gravity. $f(m)$: Mass function. Cycle: Number of cycles of the third body observed. $M_{12} \sin^3 i$: Minimum mass of the contact pair. i: Orbital inclination of the contact pair. M_{12}: Mass of the contact pair. M_3: Minimum mass of the third component. π: Parallax of the system. α: Estimated angular separation of the third component. ΔV_0: Mean difference in radial velocities. A: Full amplitude of the systemic velocity and of the $O - C$ changes, as predicted by LITE. The superscript "f" on P_3 or e_3 means that the parameter was fixed at an optimum value. For SW Lac we give separate solutions for the third and fourth components. References are given only for stars previously known or suspected to display LITE or cyclic period variations.

References.—(1) Borkovits & Hegedus 1996; (2) Demircan et al. 1993; (3) Pribulla et al. 2000; (4) Pribulla et al. 1999a; (5) Yakut et al. 2003; (6) Kim et al. 2003; (7) Pribulla et al. 1999b; (8) Hobart et al. 1998; (9) Samec et al. 2004; (10) Erdem & Özkardes 2004; (11) Pribulla & Vaňko 2002.

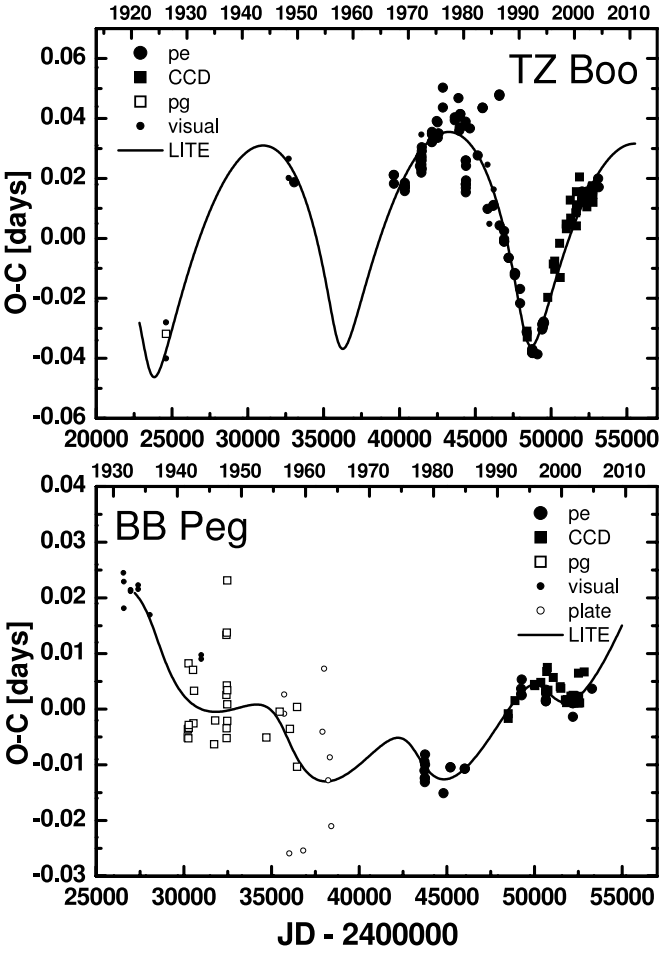

FIG. 5.—Two illustrative examples of the LITE solutions: a relatively reliably solved case for TZ Boo and a marginal detection for BB Peg. The lower horizontal axis gives the Julian Date, and the upper horizontal axis gives the year. The vertical axis gives $O - C$ residuals from an arbitrarily selected linear ephemeris. The values of $O - C$ are plotted with different symbols according to the observation type from which the instant of minimum was derived ("CCD," CCD observation; "pe," photoelectric photometry; "pg," several photographic plates; "visual," visual estimates; and "plate," the time of the minimum was crudely evaluated from the epoch of a photographic plate when the system appeared to be faint).

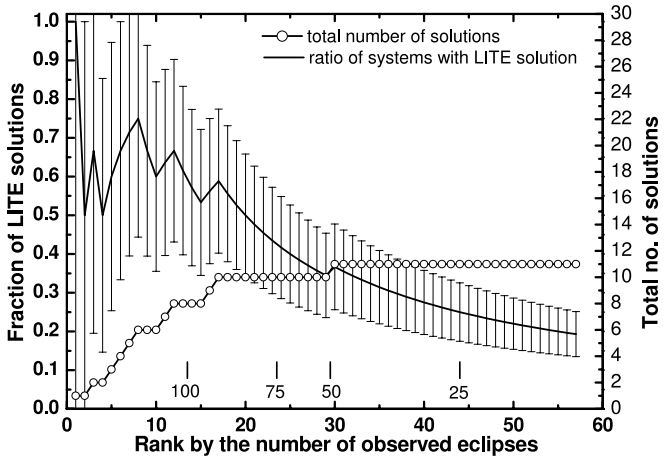

FIG. 6.—Fraction of binaries having LITE solutions with respect to the rank of the system, evaluated as the (decreasing) number of available eclipse timings. The error bars give the 1 σ Poissonian uncertainty. The vertical markers with numbers 100, 75, 50, and 25 indicate limits for the available numbers of CCD and *pe* minima (derived from CCD and photoelectric photometry, respectively) for the LITE solutions. The connected circles and the right axis show the number of systems with LITE solutions for a given rank; this number increases slowly beyond the rank of 20, which means that the detection is heavily biased by the number of available data. The figure suggests a relatively high incidence of multiplicity among the 20 best-studied systems.

the binary. Predicted mean separations for several systems (e.g., AB And, CK Boo, and V566 Oph) are accessible to speckle or direct detection. In fact, CK Boo was independently detected as a visual double during CFHT observations (§ 3.2), while a UV excess may indicate the existence of a white dwarf in the system (Krzesinski et al. 1991).

SW Lac requires special attention, as this may be a quadruple system. The first consistent LITE solution (Pribulla et al. 1999a) was not stable and could not fully explain the behavior of older minima. The multiplicity of the system was clearly seen in the spectra of Hendry & Mochnacki (1998). We have found it to be well separated in the CFHT *K*- and *H*-band adaptive optics observations (§ 3.2), with the third component too far on the sky to cause the observed LITE.

Detection of the LITE obviously depends on the number of available minima, although other factors, such as their temporal distribution, are also important. Thus, systems can be ranked according to this number, which reflects our chances to detect a cyclic period change. In Figure 6 the fraction of LITE-detected multiple systems is plotted with respect to the rank of the system, sorted according to the number of available minima times. It is obvious that the detection of multiple components among the studied systems is strongly dependent on the availability of data. For the first best-observed 20 systems, the multiplicity rate appears to be as high as about 60% ± 17%. It should be noted that most of those systems are northern hemisphere ones, as too few eclipses have been observed for southern contact binaries to permit LITE studies. We return to the point of the disparity between the hemispheres in the conclusions of this paper (§ 7).

The chance of detecting a third body by the LITE is restricted to periods from a few years (where the $O - C$ amplitudes are small) to several tens of years by the available span of the data; indeed, most systems in Table 5 have periods of about 30 yr. If the third component is the dominant source of light, it can reduce the photometric amplitude of the eclipsing pair (e.g., the case of TU UMi; Pych & Rucinski 2004), making determination of the eclipse moments very imprecise or even entirely impossible. In view of this observational bias, the 60% incidence of triple systems may be considered as possibly a low limit to an even higher value.

In Table 1 the resulting LITE status (Flag 6) is coded as follows: "D" for a stable solution, "S" for a not fully stable solution and/or less than 1.5 cycles of P_3 covered, "N" for no detection, and "–" for too few minima or less than 10 yr of CCD or *pe* observations. In our view, the LITE is almost certainly present in AB And, VW Cep, AK Her, SW Lac, XY Leo, and AH Vir.

5.2. *The Period-Color Relation and the Color Index Peculiarity* (*Flag 7*)

The period-color relation for contact binary stars was discovered observationally by Eggen (1961, 1967) and was used later for various theoretical investigations of these systems. The relation is a consequence of contact binaries being MS objects, with all implied correlations between the mass, effective temperature, and radius, and hence the size and thus the period. Observationally, the relation is a very useful tool in recognizing contact binaries in deep variability surveys and, together with the luminosity calibration $M_V = M_V(\log P,\ B - V)$ (Rucinski 1994, 1998, 2000), it forms a powerful discriminator for identifying contact binaries among short-period variable stars. The color index $B - V$ can be

replaced by $V-I$ or any other index; an unpublished $V-K$ calibration also exists (S. M. Rucinski 2006, in preparation).

As pointed out before (Rucinski 1997, 1998, 2002b), the period-color relation must have a short-period, blue envelope (SPBE). Its locus corresponds to the zero-age MS of the least evolved stars when it is applied to stars in contact and expressed in terms of the period and a color index. The evolution and expansion of components can lead to a lengthening of the period and a reddening of the color index; reddening may be also be caused by interstellar extinction. Thus, one does not expect contact binaries to appear blueward of the SPBE. Yet, some close binaries do show up there.

Rucinski (1998) suggested a simple approximation to the SPBE, $(B-V)=0.04\,P^{-2.25}$, and an explanation for the blue outliers as noncontact stars, possibly Algol-type and β Lyrae eclipsing binaries with a blue component dominating in the combined color index; a lowered metallicity may also explain some of the blue deviations (Rucinski 2000). However, some of the blue outliers may be multiple systems, with the color index peculiarity caused by a blue third star.

The period-color relation for 151 contact binaries brighter than $V_{\max}=10$ with the $B-V$ data from Tycho-2 is shown in Figure 7. One can immediately see that several systems are substantially bluer than the SPBE. Some of them are indeed known triple systems (e.g., V867 Ara and KP Peg). The most deviating systems, and the strongest cases in which to suspect the presence of an early-type component, are V445 Cep and V758 Cen.

We are very much aware of the possibility of overinterpreting the blue deviations in Figure 7, so we do not claim any detections here and point to only some systems as suspected cases of multiplicity. This is marked by the flag "S" in Table 1 for cases in which the color index deviates by more than 1 σ from the SPBE line. Systems not included in Tycho-2 are given the "–" flag. "N" signifies no detection.

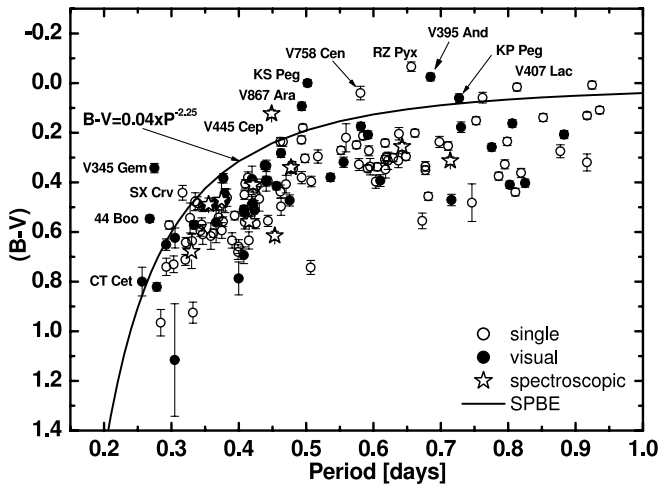

FIG. 7.—Period-color relation for contact binaries brighter than $V_{\max}=10$ appearing in the Tycho-2 catalog (*circles*). The filled circles show the known visual systems, while known spectroscopic triples are marked by stars. The solid line gives a simple approximation to the SPBE, as discussed in the text; for contact binaries, the SPBE has a meaning similar to that of the zero-age MS. Systems above and to the left of the SPBE may have blue companions.

5.3. *X-Ray Emission* (*Flag 8*)

Contact binary stars consist of solar-type stars spun into very rapid rotation by tidal forces. As a consequence, they are very active and show elevated chromospheric and coronal activity. An extensive body of data exists on their X-ray emission (Stepień et al. 2001) and, in particular, on the correlation of the X-ray coronal emission with the two most relevant parameters, the effective temperature $T_{\rm eff}$ and the orbital period P; the former controls the depth of the convective zone, while the latter controls the amount of vorticity available for the generation of magnetic fields. A convenient distance-independent quantity is the ratio of the apparent X-ray and bolometric fluxes, $f_{\rm X}/f_{\rm bol}$. It expresses the X-ray "efficiency" of how much of the total available energy is channeled into the X-rays. The value of $f_{\rm bol}$ can be estimated from the visual magnitude of the star by using the bolometric correction BC($T_{\rm eff}$). Unfortunately, many fainter binaries still do not have any standardized (e.g., *UBV*) photometric data to estimate even an approximate value of $T_{\rm eff}$. Therefore, to use a homogeneous and simple treatment, we used the shifted SPBE relation (by subtracting 0.2 mag) to estimate an approximate value of the $B-V$ color index from the orbital period (see Fig. 7); because the bolometric correction changes very little between the A0 and G5 spectral types and we are looking for order-of-magnitude effects in $f_{\rm X}/f_{\rm bol}$, the resulting approximation is adequate. The X-ray fluxes were estimated using the procedure described in Stepień et al. (2001) from the observed *ROSAT* All-Sky Survey (RASS) X-ray count rate and the hardness ratio (between the 0.1–0.4 and 0.5–2.0 keV bands). The measured X-ray fluxes were corrected for the background count rate. In the computation of bolometric fluxes we took 2.5×10^5 ergs cm^{-2} s^{-1} as a flux for $M_{\rm bol}=0$. The bolometric corrections were interpolated in the table given by Popper (1980).

We used the RASS catalog (Voges et al. 1999, 2000) to find $f_{\rm X}$ in the 0.1–2.4 keV band for all contact binaries of our sample. Although the catalog contains its own cross identifications, after realizing many omissions we cross-correlated the RASS catalog data with the International Celestial Reference System coordinates taken from SIMBAD for all CCBS systems. The angular separation of 36″ was taken as a limit for detection. Six additional distant sources identified in SIMBAD have also been included. Although not all detections are secure due to the relatively low pointing precision (typically 10″–20″), most identifications are unambiguous, as most of the targets do not have any other objects within 0.°5. Some binaries of our sample were not detected, providing a useful upper limit on $f_{\rm X}/f_{\rm bol}$, derived from the assumed detection threshold of 0.01 counts s^{-1}. To better define the lower envelope of the upper limits on $f_{\rm X}/f_{\rm bol}$, we also added systems fainter than $V_{\max}=10$ mag from CCBS. The results are shown in Figure 8.

Following the previous investigations (Cruddace & Dupree 1984; Stepień et al. 2001), we expected the ratio $f_{\rm X}/f_{\rm bol}$ to show a weak dependence on the binary orbital period close to a saturation limit at $f_{\rm X}/f_{\rm bol}\simeq10^{-3}$. However, the scatter in Figure 8 is large, with some deviations reaching factors of 10 or 100 times from the average. We argue that companions to contact binaries may be the cause of these large deviations and that the deviations may go both ways: (1) when an early-type contact binary has an M dwarf companion or, particularly, a *binary* M dwarf companion (as in the case of XY Leo), then $f_{\rm X}/f_{\rm bol}$ can be strongly elevated, but (2) when the contact binary is of solar or later spectral type, its magnetically inactive early-type companion may reduce the value of $f_{\rm X}/f_{\rm bol}$ (as in the cases of 44 Boo or V752 Mon). Indeed, this is exactly what we do see in Figure 8 for the known triple systems: (1) In the lower left corner, a few systems with a relatively low flux ratio are in majority triple systems in which the X-ray flux is diluted by the dominant early-type, single star (e.g., V345 Gem). (2) The majority of short-period systems with high relative X-ray fluxes are triple systems; in some cases a late-type, binary, BY Dra–type companion provides most of the X-ray flux (e.g., XY

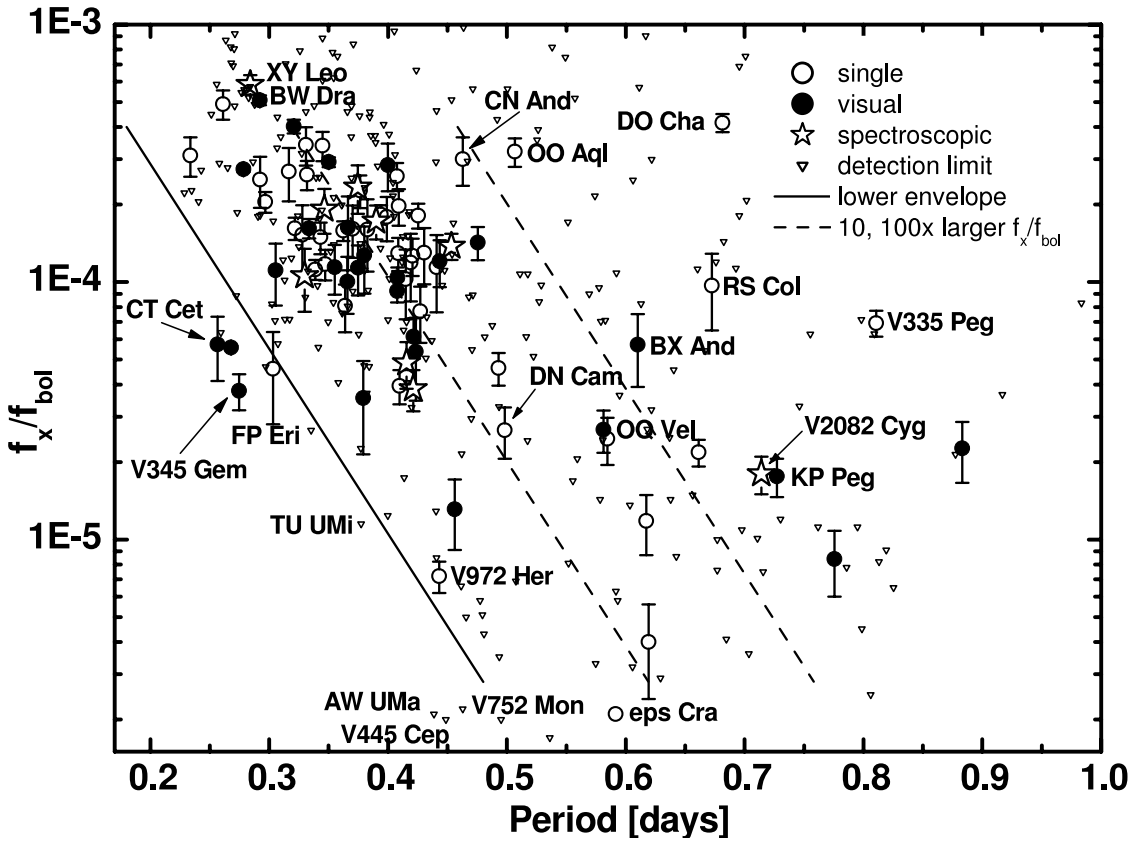

FIG. 8.—Ratio of the apparent X-ray and bolometric fluxes, f_X/f_{bol} vs. orbital period. The ratio f_X/f_{bol} is expected to scale with the orbital period, with the short-period systems being on average more X-ray active. The solid line gives the approximate locus (selected to encompass most of the systems) of the LXLE in X-rays, while the dashed lines give the same envelope shifted up by 10 and 100 times. The f_X/f_{bol} points in this figure are based on detections (*circles*) and the upper limits (*triangles*) for all contact binaries in the RASS. The presence of companions is expected to modify the flux ratio by enhancing it when companions are active M dwarfs and diminishing it when companions are early A/F-type stars. The filled circles denote members of known visual binaries, and stars give spectroscopic detections (here we added two spectroscopic detections, XY Leo and ET Leo, with astrometric indication).

Leo). (3) Several early-type, long-period contact systems, expected to be practically inactive, show enhanced X-ray flux (V335 Peg, DO Cha, or RS Col), which may indicate that they host a late-type, active companion.

The f_X/f_{bol} ratio should be used as an indicator of multiplicity with considerable caution, particularly in view of the large number of upper limits to the X-ray flux values. However, it may be highly indicative in individual cases already signaled by other techniques. In Figure 8 we marked a line delineating the low X-ray luminosity envelope (LXLE) of the observed f_X/f_{bol} ratios. The line was selected rather arbitrarily to encompass most of the systems. Systems with f_X/f_{bol} values >100 times above the LXLE are marked in Table 1 by "L," for "late-type companion." Similarly, late-type contact systems with abnormally low emission, those below the LXLE, are marked by "E," for "early-type companion." For periods longer than 0.5 days, the LXLE is not defined because such contact binaries of spectral type early F or earlier are not expected to show any detectable X-radiation.

5.4. *Lunar Occultations*

The high-speed photometry of lunar occultations can lead to detection of multiple components, and the technique is widely used (Richichi et al. 2002; Kazantseva & Osipov 2002). An angular detection limit for bright binaries, given by the Moon-limb diffraction angular scale, is about 2 mas (Warner 1988). For faint stars, this limit is modified by the diameter of the telescope through the photon noise in very short integrations used in the high-speed photometry. Due to the apsidal motion of its orbit, the Moon can occult about 9% of the sky. From among 391 contact binary stars in the electronic version of CCBS (Pribulla et al. 2003), 26 lie within the path of the Moon ($b = \pm 5^\circ 9'$ around the ecliptic).

Among the systems in Table 1, the best candidates for occultations are the bright systems AQ Psc ($V = 8.68$, $b = -0^\circ.867$), V4408 Sgr ($V = 8.29$, $b = +2^\circ.907$), and V781 Tau ($V = 8.90$, $b = +3^\circ.541$). Somewhat fainter but interesting systems are CX Vir, V1123 Tau, AP Leo, AM Leo, UZ Leo, XY Leo, RZ Tau, TX Cnc, VZ Lib, AH Aur, and CT Tau. The binaries that can be studied using the Moon-occultation technique are marked by "M" in the column headed "Moon" in Table 1. So far only the quadruple system XY Leo was observed (Evans et al. 1986), but with a negative result.

5.5. *The Third Light in Light-Curve Solutions*

The light-curve analysis sometimes indicates a need of a "third light" as an additive term in the overall brightness budget. A third component to a binary system can be such a third light, but light curves are described by so many parameters that this is frequently an unreliable indicator of multiplicity. Certainly, for light curves of partially eclipsing spherical stars in only one band, the third light is just an "easy escape" to obtain a solution, but for contact binaries its physical reality becomes even more dubious because of a more complex geometry.

Light-curve synthesis solutions indicating a need for a third light usually show a tight correlation of the third light with the inclination angle and the mass ratio. Even for the best-constrained

solutions of contact binaries showing total eclipses, where inner eclipse contacts can be well defined and the mass ratio can be determined solely from light curves (Mochnacki & Doughty 1972), a correlation between mass ratio and the third light remains. An example is the case of EF Dra, for which the light curve indicated $q_{\rm phot} = 0.10$ (Robb & Scarfe 1989), while the spectroscopic mass ratio is $q_{\rm spec} = 0.16$ (Lu & Rucinski 1999). Usually, without spectroscopic determination of the mass ratio it is hardly possible to detect third light from light curves with the usual photometric precision of $\approx$0.01 mag. The situation improves when the third component has a markedly different spectral type than the binary and when photometry is available in several bandpasses; then, instead of uncorrelated values of L_3 in each band, the proper approach is to use the radius and temperature of the third star. At this time we feel that we have no clear case of a third light in any of the contact binaries of our sample.

5.6. *Precession of the Orbital Plane*

A close and massive third body orbiting a binary system can cause precession of the orbital plane and an apsidal motion of the close pair. The largest dynamical effects are expected for contact binaries, which contain the least angular momentum among all binaries. Precession of the orbital plane in an eclipsing binary will result in changes of its orbital inclination and thus changes of the photometric amplitude of the eclipses. The practical use of the method consists of a comparison of high-quality light curves obtained over long time intervals in search of amplitude variations.

The precession period depends on the period ratio P_3^2/P_{12} and (weakly) on the ratio of the outer orbit angular momentum to the total invariable angular momentum and on the ratio of the total triple system mass and that of the third body mass. The nodal period is, to the first order (see eq. [27] in Söderhjelm 1975), given by

$$P_{\rm node} = \frac{4}{3}\frac{m_{123}}{m_3}\frac{P_3^2}{P_{12}}\left(1-e_3^2\right)^{3/2}\frac{L_3}{L}\sec j, \qquad (2)$$

where m_{123} is the total mass, L is the total invariable angular momentum of the triple system, L_3 is the angular momentum of the outer orbit, and j is the relative inclination of the orbits.

Systematic changes in the eclipse depth indicating orbital precession have been observed in several detached binaries (Mayer et al. 2004). However, none of the contact binaries has shown this effect, although many are observed on a routine basis. Chances to see the effect are high due to (1) the very low angular momentum of a typical contact binary, (2) its short orbital period, and, usually, (3) a low total mass of the eclipsing pair. Any adverse effects of the photometric system mismatch are also minimized thanks to both components having the same temperature so that the light-curve amplitude is almost independent of the wavelength used, permitting comparison of curves obtained in different photometric systems.

6. STATISTICS AND RESULTS

We have carefully inspected our list of contact binaries brighter than $V_{\rm max} = 10$ and with periods shorter than 1 day to establish all cases that appear to indicate multiplicity. The last column of Table 1 contains the letter code "Y" for cases of sufficient information to claim that a contact binary is indeed part of a multiple system. Our decision was based on a combined "weight," as determined from individual detection techniques, equal to or exceeding the value of 1.0. In adding the weights we used a weight of 1.0 for individual unquestionable detections and a weight of 0.5 for suspected cases. Although this approach produces nonsubjective and repeatable results, we feel that not all cases for accepted detections are equally valid. We comment on individual cases requiring explanation in Table 3.

We see 64 triple systems among the 151 objects of our sample, giving a nominal lower limit to the frequency of triple systems of 42% $\pm$ 5%. This result is for both hemispheres, which have not been equally well surveyed to apply all available methods, with the southern hemisphere contributing very few binaries to the final statistics. Indeed, if not for the *Hipparcos* mission, which discovered a few visual binaries containing contact binaries (e.g., V867 Ara and CN Hyi), there would be almost no known visual binary detections in the southern sky. While in the northern sky ($\delta > 0$), using all available techniques, we see 52 triple systems among 88 objects, giving a frequency of 59% $\pm$ 8%, the southern sky yields only 12 systems out of 63, corresponding to 19% $\pm$ 6%. The reason is the low number of contact binaries discovered so far in the south, a meager volume of photometric data even for the known ones (some binaries were observed for the last time half a century ago!), a lack of any spectroscopic support, and a short time base for techniques requiring accumulation over time (such as visual orbits, proper motions, and LITE).

In principle, our result on the low limit to the frequency of triple systems containing contact binaries of 59% $\pm$ 8% should be compared with control samples for single stars and for wider binaries. Such samples are only now being created with the particularly strong contributions of Tokovinin (1997, 2004). However, the data are fragmentary and—even for bright, nearby, single stars—heavily biased by the distance and brightness selection effects. Tokovinin (2004) found that among the 18 dwarfs closest to 8 pc, 5 exist in multiple systems, giving a frequency of 28%. However, a deeper search based on 3383 dwarfs to 50 pc (Tokovinin 2004) yielded only 76 multiple systems, 2.2%, with the heavy bias against discovery setting in for systems beyond 10 pc. While our final conclusion is that triple systems are very frequent for the contact binaries, we note that several of our techniques are different from those of Tokovinin and are distance-independent; this may explain our high result when compared with that of Tokovinin (2004), in spite of the fact that our targets are spread in distance from 13 pc to hundreds of parsecs.[7] The situation appears to be different for binaries. Tokovinin (1997) found that the frequency of triplicity and multiplicity among spectroscopic binary stars with orbital periods shorter than 10 days appears to be high: as many as 43% $\pm$ 8% (26 out of 61) among nearby (within 100 pc), low-mass (0.5–1.5 $M_\odot$), spectroscopic binaries cataloged in Batten et al. (1989) have known tertiary components. Our estimate for the northern hemisphere contact binaries of 59% $\pm$ 8% is consistent with Tokovinin's results within the statistical errors but is slightly higher. This may indicate that the frequency keeps on increasing for shorter periods but that the underlying physical causes for periods $P < 10$ days may be similar.

We note that the main route for detection of companions is the small angular separation on the sky. Among the 64 positive detections, 46 systems are known visual, previously cataloged WDS and *Hipparcos* binaries or new discoveries of the new CFHT, adaptive optics infrared observations; the latter nicely complemented the extant data for M dwarf companions at angular separations of about 0.″1 to a few arcseconds. In turn, most of the spectroscopic detections have been of systems already known as visual binaries; spectroscopy can, however, help in determining the physical characteristics of the companion and firm up individual cases.

[7] The distance to the closest contact binary, 44 Boo, is 12.77 pc.

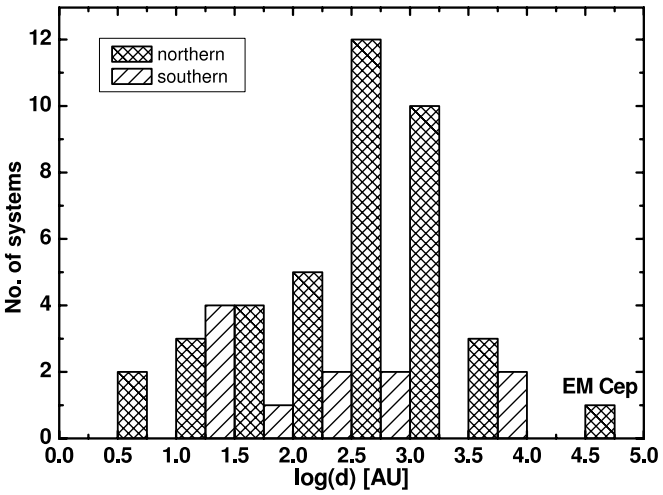

FIG. 9.—Projected separations in astronomical units for all systems with $V_{max} < 10$ that have available astrometric data, shown separately for both hemispheres (relative to the celestial equator). The large disparity in numbers is directly visible. EM Cep (the only system in the bin with $4.5 < \log d < 5$), sometimes considered to be in a visual binary with a very large separation, is probably not a physically bound system (see the text).

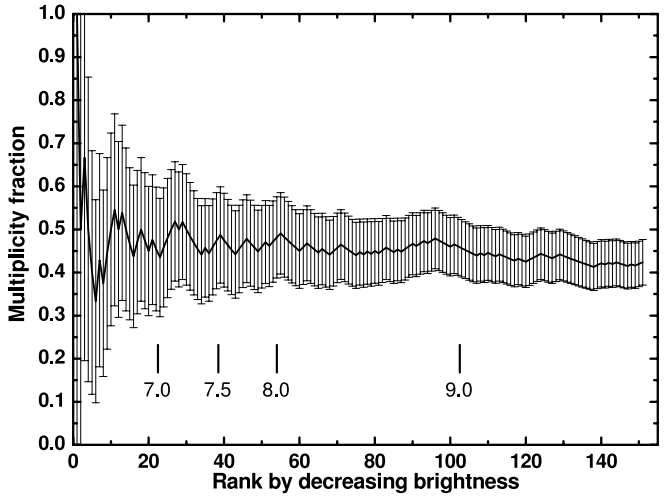

FIG. 10.—Fraction of contact binaries having an additional component. The systems have been ranked according to the maximum brightness. The fraction is a cumulative one in the sense that it corresponds to a given rank and to ranks below it. The corresponding magnitude limits are marked by the vertical markers. Note that systems fainter than $V_{max} \simeq 9$ appear to show a bias of a decreasing multiplicity fraction.

The visual technique, combined with the parallax data, permits us to evaluate projected physical separations between the companions. The projected separations are moderate and are distributed in the range between 6 and 10^4 AU, or between 2.9×10^{-5} and 0.049 pc (Table 1).[8] Figure 9 shows a histogram of the projected separations. The distribution may partly reflect observational biases, but it does show that the separations are much smaller than the typical distances between stars in the solar neighborhood of about 1 pc. Thus, even the widest pairs with angular separations of several tens of arcseconds can be regarded as gravitationally bound; an example is AW UMa, where for the angular separation of 67″ the projected separation is 4400 AU. But, physically, can these multiples be evolutionarily connected at such disparate separations, ranging between stellar sizes and thousands of astronomical units? Can the Kozai cycle work at such large distances, or do we see now only the results of it acting well in the past? Answers to these exciting questions are beyond the scope of this paper.

7. FUTURE WORK AND CONCLUSIONS

The approach that we used in this paper was a straightforward one: we simply counted contact binaries that appeared to have companions. We totally disregarded the important matter of *what the companions are and what would be the limitations in their detection*. Some classes of stars, such as white dwarfs or neutron stars, would require utilization of special techniques; some classes may be entirely undetectable. We leave these issues open for future investigations of this series.

The use of several different observational techniques was certainly useful, as none gives unquestionable proof of multiplicity and each has its own biases and limitations. We used too many techniques to analyze the selection effects of each; such in-depth studies of biases for each technique would inflate the study and would probably not be warranted at this preliminary stage. But we know that biases are important: taking the astrometric data for the 50 best-observed systems in the whole sky brighter than $V_{max} = 10$ (§ 3; Fig. 2), we see a frequency of 40% ± 9%, but this number would rise to 46% ± 10% if we disregarded the magnitude limit and argued that objects best-observed astrometrically would provide an even more reliable sample (indeed, there are many bright systems with poor data). The sky location is also important: for the northern subsample of astrometrically well-observed stars to $V_{max} = 10$, the frequency increases from 40% ± 9% to 50% ± 10%. Similarly, entirely independent indications for the 20 best observed systems for the LITE suggest 60% ± 17%; among those LITE solutions, only two are for nominally southern systems, although both were observed from the north (ER Ori with $\delta = -8^{\circ}.5$ and UX Eri with $\delta = -6^{\circ}.9$).

The most obvious observational bias caused by the brightness of the system is demonstrated in Figure 10, where the fraction of detections is plotted for all systems brighter than the given magnitude rank. While for systems brighter than $V_{max} = 9$ mag we see an almost constant fraction of multiples, there is a small but definite decrease of detections for fainter systems.

In addition to in-depth analyses of selection effects and biases of individual techniques, we issue the usual plea to the observers: more data are needed! What are particularly needed are photometric data in standard systems. If not for the *Hipparcos* mission, which led to many discoveries of contact binaries, and if not for the photometric part of the Tycho project, many contact binaries would be unknown or without the most elementary data on color indices. All contact systems also require radial velocity spectroscopic support. The situation with the southern sky is particularly grave. There exists no spectroscopic survey similar to that being conducted now for short-period northern binaries at DDO, so even relatively bright southern contact binaries (TY Men, DE Oct, MW Pav, CN Hyi, WY Hor, V386 Pav, etc.) still await spectroscopy or even conventional precision photometry. Very few southern binaries are followed over time to provide LITE information. For many binaries, the last datum on the moment of minimum is the *Hipparcos* T_0.[9] Interesting southern systems

[8] We exclude EM Cep and AH Cnc, which are members of the open cluster and whose projected separations are 49,700 and 24,000 AU, respectively. We do not consider these systems as multiple ones.

[9] This remark unfortunately also applies to some northern binaries that do not happen to be popular.

omitted by *Hipparcos* (e.g., BR Mus, TV Mus, and ST Ind) frequently have the last minima obtained a quarter or half a century ago. We also point out that the technique of lunar occultations still remains to be fully used, as it can provide an angular resolution of about 2 mas and thus can be a powerful tool for the detection of close visual companions.

We conclude with a summary of our results. Our best estimate of the lower limit to the triple star incidence among contact binaries appears to be 59% ± 8%, as based on the northern sky to $V_{\max} = 10$. We know that this limit may rise as suspected cases are analyzed more thoroughly. If, in addition to the unquestionable detection of 64 multiple systems among 151 targets over the whole sky, all 24 suspected cases in Table 1 were included as detections, then the frequency for the whole sky would increase from 42% ± 5% to 56% ± 6%, while that for the northern hemisphere alone would reach 72% ± 9%. Our results are consistent with those for the magnitude-complete *Hipparcos* sample to $V_{\max} = 7.5$ (Rucinski 2002b), with 17 multiples among 35 systems (48% ± 12%), although for that sample a large fraction of all systems were newly discovered eclipsing binaries with currently incomplete data. Remembering that we could evaluate only a lower limit to the frequency of triple systems and that some multiple systems are beyond reach of any current technique of detection, this number is not far from one indicating a possibility that all contact binaries originated in multiple systems.

Thanks are expressed to the anonymous reviewer who very carefully read the first version of the paper and suggested very useful changes to it. Support from the Natural Sciences and Engineering Council of Canada to S. M. R. is acknowledged with gratitude. The travel of T. P. to Canada has been supported by an IAU Commission 46 travel grant and Slovak Academy of Sciences VEGA grant 4014. T. P. appreciates the hospitality and support of the local staff during his stay at DDO. This research made use of the SIMBAD database, operated at the CDS, Strasbourg, France, and accessible through the Canadian Astronomy Data Centre, which is operated by the Herzberg Institute of Astrophysics, National Research Council of Canada. This research also made use of the Washington Double Star Catalog maintained at the US Naval Observatory.

REFERENCES

Afsar, M., Heckert, P. A., & Ibanoglu, C. 2004, A&A, 420, 595
Applegate, J. H. 1992, ApJ, 385, 621
Barden, S. C. 1987, ApJ, 317, 333
Bate, M. R. 2004, Rev. Mex. AA Ser. Conf., 21, 175
Batten, A. H., Fletcher, J. M., & MacCarthy, D. G. 1989, Publ. Dominion Astrophys. Obs., 17, 1
Borkovits, T., & Hegedus, T. 1996, A&AS, 120, 63
Chambliss, C. R. 1992, PASP, 104, 663
Cruddace, R. G., & Dupree, A. K. 1984, ApJ, 277, 263
D'Angelo, C., van Kerkwijk, M., & Rucinski, S. M. 2006, AJ, in press (Paper II)
Demircan, O., Akalin, A., & Derman, E. 1993, A&AS, 98, 583
Duerbeck, H. W. 1997, Inf. Bull. Variable Stars, 4513, 1
Eggen, O. J. 1961, R. Obs. Bull., 31, 101
———. 1967, MmRAS, 70, 111
Eggleton, P. P., & Kiseleva-Eggleton, L. 2001, ApJ, 562, 1012
Erdem, A., & Özkardes, B. 2004, Inf. Bull. Variable Stars, 5496, 1
Evans, D. S., McWilliam, A., Sandmann, W. H., & Frueh, M. 1986, AJ, 92, 1210
Fabricius, C., Høg, E., Makarov, V. V., Mason, B. D., Wycoff, G. L., & Urban, S. E. 2002, A&A, 384, 180
Fabricius, C., & Makarov, V. V. 2000, A&A, 356, 141
Genet, R. M., & Smith, T. C. 2004, AAS Meeting, 205, 1802
Goecking, K. D., Duerbeck, H. W., Plewa, T., Kaluzny, J., Schertl, D., Weigelt, G., & Flin, P. 1994, A&A, 289, 827
Hadrava, P. 2004, in ASP Conf. Ser. 318, Spectroscopically and Spatially Resolving the Components of Close Binary Stars, ed. R. W. Hilditch, H. Hensberge, & K. Pavlovski (San Francisco: ASP), 86
Hendry, P. D., & Mochnacki, S. W. 1998, ApJ, 504, 978
Hershey, J. L. 1975, AJ, 80, 662
Hill, G., Fisher, W. A., & Holmgren, D. 1989, A&A, 211, 81
Hobart, M. A., Peña, J. H., & Dela Cruz, C. 1998, Ap&SS, 260, 375
Høg, E., et al. 2000, A&A, 355, L27
Hrivnak, B. J. 1988, ApJ, 335, 319
Irwin, J. B. 1959, AJ, 64, 149
Kalimeris, A., Rovithis-Livaniou, H., & Rovithis, P. 2002, A&A, 387, 969
Kazantseva, L. V., & Osipov, E. O. 2002, KFNT, 18, 179
Kharchenko, N. V., Piskunov, A. E., Röser, S., Schilbach, E., & Scholz, R. D. 2005, A&A, 438, 1163
Kim, C. H., Lee, J. W., Kim, H. I., Kyung, J. M., & Koch, R. H. 2003, AJ, 126, 1555
King, D. J., & Hilditch, R. W. 1984, MNRAS, 209, 645
Kirkpatrick, J. D., Henry, T. J., & McCarthy, D. W. 1991, ApJS, 77, 417
Kiseleva, L. G., Eggleton, P. P., & Mikkola, S. 1998, MNRAS, 300, 292
Kozai, Y. 1962, AJ, 67, 591
Kreiner, J. M., Kim, C. H., & Nha, I. S. 2001, An Atlas of ($O - C$) Diagrams of Eclipsing Binary Stars (Cracow: Wydawnictwo Naukowe Akad. Pedagogicznej)
Krzesinski, J., Pajdosz, G., Mikolajewski, M., & Zola, S. 1991, Ap&SS, 184, 37
Lu, W., & Rucinski, S. M. 1999, AJ, 118, 515
Lu, W., Rucinski, S. M., & Ogloza, W. 2001, AJ, 122, 402
Mason, B. D., Hartkopf, W. I., Holdenreid, E. R., & Rafferty, T. 2001a, AJ, 121, 3224
Mason, B. D., Wycoff, G. L., Hartkopf, W. I., Douglass, G. G., & Worley, C. E. 2001b, AJ, 122, 3466
Mason, B. D., et al. 1999, AJ, 117, 1890
Mayer, P., Pribulla, T., & Chochol, D. 2004, Inf. Bull. Variable Stars, 5563, 1
Mochnacki, S. W., & Doughty, N. A. 1972, MNRAS, 156, 51
Payne-Gaposhkin, C. 1941, Publ. AAS, 10, 127
Perryman, M. A. C., et al. 1997, The *Hipparcos* and Tycho Catalogues (ESA SP-1200; Noordwijk: ESA)
———. 1980, ARA&A, 18, 115
Pourbaix, D., Platais, I., Detournay, S., Jorissen, A., Knapp, G., & Makarov, V. V. 2003, A&A, 399, 1167
Pribulla, T., Chochol, D., Heckert, P. A., Errico, L., Vittone, A. A., Parimucha, Š., & Teodorani, M. 2001, A&A, 371, 997
Pribulla, T., Chochol, D., & Parimucha, Š. 1999a, Contrib. Astron. Obs. Skalnaté Pleso, 29, 111
Pribulla, T., Chochol, D., Rovithis-Livaniou, E., & Rovithis, P. 1999b, A&A, 345, 137
Pribulla, T., Chochol, D., Tremko, J., & Kreiner, J. M. 2005, in ASP Conf. Ser. 335, The Light-Time Effect in Astrophysics, ed. C. Sterken (San Francisco: ASP), 103
Pribulla, T., Chochol, D., Tremko, J., Parimucha, Š., Vaňko, M., & Kreiner, J. M. 2000, Contrib. Astron. Obs. Skalnaté Pleso, 30, 117
Pribulla, T., Kreiner, J. M., & Tremko, J. 2003, Contrib. Astron. Obs. Skalnaté Pleso, 33, 38
Pribulla, T., & Vaňko, M. 2002, Contrib. Astron. Obs. Skalnaté Pleso, 32, 79
Pribulla, T., et al. 2006, AJ, submitted
Pych, W., & Rucinski, S. M. 2004, Inf. Bull. Variable Stars, 5524, 1
Pych, W., et al. 2004, AJ, 127, 1712
Qian, S., He, J., Xiang, F., Ding, X., & Boonrucksar, S. 2005, AJ, 129, 1686
Richichi, A., Calamai, G., & Stecklum, B. 2002, A&A, 382, 178
Rigaut, F., et al. 1998, PASP, 110, 152
Robb, R. M., & Scarfe, C. D. 1989, Inf. Bull. Variable Stars, 3370, 1
Rucinski, S. M. 1992, AJ, 104, 1968
———. 1993, in The Realm of Interacting Binary Stars, ed. J. Sahade, G. E. McCluskey, & Y. Kondo (Dordrecht: Kluwer), 111
———. 1994, PASP, 106, 462
———. 1997, AJ, 113, 407
———. 1998, AJ, 116, 2998
———. 2000, AJ, 120, 319
———. 2001, AJ, 122, 1007
———. 2002a, AJ, 124, 1746
———. 2002b, PASP, 114, 1124
Rucinski, S. M., & Duerbeck, H. W. 1997, PASP, 109, 1340
Rucinski, S. M., & Kaluzny, J. 1982, Ap&SS, 88, 433

Rucinski, S. M., Lu, W., Capobianco, C. C., Mochnacki, S. W., Blake, R. M., Thomson, J. R., Ogloza, W., & Stachowski, G. 2002, AJ, 124, 1738
Rucinski, S. M., Lu, W. X., & Shi, J. 1993, AJ, 106, 1174
Rucinski, S. M., et al. 2003, AJ, 125, 3258
———. 2005, AJ, 130, 767
Samec, R. G., Faulkner, D. R., & Williams, D. B. 2004, AJ, 128, 2997
Söderhjelm, S. 1975, A&A, 42, 229
———. 1999, A&A, 341, 121
Stepień, K., Schmitt, J. H. M. M., & Voges, W. 2001, A&A, 370, 157
Struve, O. 1949, ApJ, 109, 436
Struve, O., & Gratton, L. 1948, ApJ, 108, 497
Struve, O., Horak, H. G., Canavaggia, R., Kourganoff, V., & Colacevich, A. 1950, ApJ, 111, 658
Struve, O., & Zebergs, V. 1959, ApJ, 130, 789
Tholine, J. E. 2002, ARA&A, 40, 349
Tokovinin, A. A. 1997, A&AS, 124, 75
———. 2004, Rev. Mex. AA Ser. Conf., 21, 7
Voges, W., et al. 1999, A&A, 349, 389
———. 2000, IAU Circ., 7432, 1
Walker, R. L. 1973, Inf. Bull. Variable Stars, 855, 1
Warner, B. 1988, High-Speed Astronomical Photometry (Cambridge: Cambridge Univ. Press)
Yakut, K., Ibanoglu, C., Kalomeni, B., & Demirgenci, O. L. 2003, A&A, 401, 1095
Zhai, D., & Lu, W. 1989, Acta Astrophys. Sinica, 9, 208
Zinnecker, H. 2002, in ASP Conf. Ser. 285, Modes of Star Formation and the Origins of Field Populations, ed. E. K. Grebel & W. Brandner (San Francisco: ASP), 131
Zinnecker, H., & Mathieu, R. D., eds. 2001, IAU Symp. 200, The Formation of Binary Stars (San Francisco: ASP)